# Accepted Manuscript

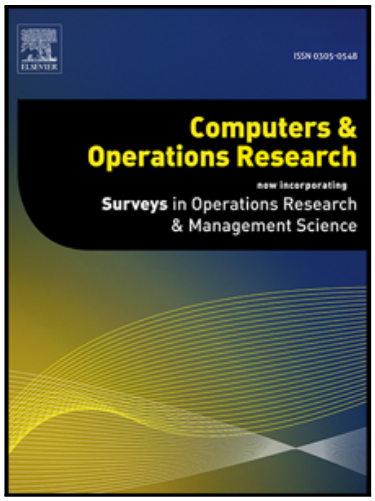


Equity portfolio management with cardinality constraints and risk parity control using multi-objective particle swarm optimization

Massimiliano Kaucic

PII: S0305-0548(19)30127-3
DOI: https://doi.org/10.1016/j.cor.2019.05.014
Reference: CAOR 4709

To appear in: *Computers and Operations Research*

Received date: 26 January 2018
Revised date: 12 April 2019
Accepted date: 16 May 2019

Please cite this article as: Massimiliano Kaucic, Equity portfolio management with cardinality constraints and risk parity control using multi-objective particle swarm optimization, *Computers and Operations Research* (2019), doi: https://doi.org/10.1016/j.cor.2019.05.014

**Highlights**

- Novel portfolio design including cardinality constraint and risk parity condition in the set of constraints.
- Variant of the multi-objective particle swarm optimization algorithm.
- Hybrid constraint-handling technique based on the constrained Pareto dominance and a repair mechanism.
- Computational in-sample and out-of-sample comparisons with the cardinality constrained portfolio optimization model.
- The proposed investment strategy presents a major control on risks without renouncing to suitable profits.

# Equity portfolio management with cardinality constraints and risk parity control using multi-objective particle swarm optimization

Massimiliano Kaucic

*Department of Economics, Business, Mathematics and Statistics, University of Trieste, Piazzale Europa 1, 34127 Trieste, Italy*

**Abstract**

The financial crisis and the market uncertainty of the last years have pointed out the shortcomings of traditional portfolio theory to adequately manage the different sources of risk of the investment process. This paper addresses the issue by developing an alternative portfolio design, that integrates risk parity into the cardinality constrained portfolio optimization model. The resulting mixed integer programming problem is handled by an improved multi-objective particle swarm optimization algorithm. Three hybrid approaches, based on a repair mechanism and different versions of the constrained-domination principle, are proposed to handle constraints. The efficiency of the algorithm and the effectiveness of the solution approaches are assessed through a set of numerical examples. Moreover, the benefits of adopting the proposed strategy instead of the cardinality constrained mean-variance approach are validated in an out-of-sample experiment.

*Keywords:* Portfolio optimization, cardinality constraint, risk parity, hybrid constraint-handling, MOPSO

## 1. Introduction

The approach developed by Markowitz in [1] models the portfolio construction process as an optimization problem involving the selection of promising assets and the allocation of capital among them. In this framework, the expected return of the portfolio is maximized while its variance, perceived as a risk for the investment, is minimized. A portfolio is efficient if it provides the maximum return for a given level of risk or, equivalently, if it has the minimum risk for a given level of desired return. Hence, the set of optimal portfolios requires the formulation and solution of a quadratic program. In the risk-return space, the set of optimal mean-variance tradeoffs forms the so-called efficient

*Email address:* massimiliano.kaucic@deams.units.it (Massimiliano Kaucic)

frontier, or Pareto front.

Several variants of the basic model have been investigated to render it more realistic ([2], [3]). Recently, it has been suggested the inclusion of a cardinality constraint that limits the number of assets to hold in the portfolio in an attempt to control costs and improve its performance [4]. The associated mixed-integer quadratic program represents the so-called cardinality constrained portfolio optimization problem (CCPOP). It has been proven to be NP-hard [5] and, consequently, the computation of the entire efficient frontier becomes computationally challenging. The various algorithms studied to solve this issue can be roughly grouped in the following two categories. From one hand, there are exact methods ([6], [7], [8]), that provide optimal solutions but, as the problem size grows, they present unmanageable computational times. From the other hand, heuristic approaches ([9], [10], [11], [12], [13], [14]), that guarantee the identification of approximate good, and sometimes optimal, solutions even for large size instances of CCPOP within reasonable time.

In the last decade, researchers have tried to tackle the CCPOP in its multi-objective form, by optimizing both objectives at the same time with the so-called multi-objective evolutionary algorithms ([15], [16], [17]). The main advantage of these procedures, with respect to single objective algorithms, is that they are able to find the efficient frontier in a single run.

From an economic point of view, the traditional Markowitz's model treats both the above and the below target returns equally, while investors are more concerned about the probability of investment returns falling below the target return. Therefore, risks are under-estimated and portfolios that are downside efficient are ruled out. An alternative approach that properly models the loss aversion of investors is the replacement of variance with a downside risk measure. Nowadays, due to the regulatory importance of quantifying large losses in banking and insurance sectors, the so-called value-at-risk (VaR) occupies a leading position as risk management tool. It is defined as the maximum loss occurring over a given period at a given confidence level. Although it is apparently simple and intuitive, VaR presents several disadvantages. Primarily, it ignores losses exceeding VaR and is not sub-additive, i.e. diversification of the portfolio may increase it [18]. In order to deal with these shortcomings, Rockafellar and Uryasev introduce the conditional value-at-risk (CVaR), which is the conditional expectation of losses above the VaR [19].

The financial crisis of 2008 pointed out two other drawbacks of the Markowitz portfolio selection model: from one hand, relying on the estimates of expected returns, the optimal portfolio may be highly unstable; from the other hand, this approach tends to provide solutions excessively concentrated on few assets, thus failing in diversifying risks. A period characterized by uncertainty has followed. Consequently, investors have moved their attention toward novel portfolio strategies able to capture risk premia at lower risk levels [20]. The management of different sources of risk involved in the investment process has thus become of primary relevance. Contrary to the Markowitz approach, risk-based strategies only encompass the risk dimension and neglect the performance one. In this manner, they do not require any explicit stock return forecasts and

take into account solely drift and changes in risk views. Risk parity is certainly one of the most promising notions in this context [21]. It is defined in terms of risk contributions, where weights are adjusted so that all assets equally contribute to portfolio risk [22]. Its theoretical properties have been studied in [23], while the empirical comparisons conducted in [24] indicate that risk parity portfolios have a lower risk than naive portfolios and have higher Sharpe ratio than the minimum variance portfolios. However, the existence and uniqueness of a solution to the risk parity portfolio selection problem can be guaranteed only in some special cases, for which ad hoc methods have been proposed in literature ([23], [25], [26], [27]). The only effective tool for the general case is represented by the use of a heuristic algorithm that is able to find approximate solutions ([28], [29]).

The mutated economic conditions of the recent years have encouraged scholars and practitioners to develop investment strategies that balance performance and risk concentration by combining aggressive active portfolios, based on the Markowitz optimization model, with more conservative risk control approaches. A first attempt in this direction is represented by [30], where a generalized risk measure is introduced that takes into account both the portfolio return and volatility. The author suggests the use of the cyclical coordinate descent algorithm [31] to solve numerically the resulting risk parity portfolio allocation problem. Feng and Palomar [32] develop a framework gathering the most used risk parity formulations present in the literature with different performance objectives, and propose the use of a successive convex optimization method as solver. An extension of the procedure, that includes asset selection, is given in [33]. The novel formulation represents portfolio cardinality as a regularization term added to the objective function.

Unlike the aforementioned studies, that tackle the portfolio selection problem by optimizing a weighted sum of the involved criteria, we develop a multi-objective optimization framework in order to generate an even spread of points that accurately represents the complete Pareto optimal set. Our approach introduces risk parity in the definition of the admissible set of the mean-variance portfolio optimization model through mixed integer constraints. Furthermore, we use a tolerance threshold to identify solutions that are approximately at parity for the cases in which optimal portfolios do not exist.

Risk parity has been usually considered in asset-class strategies, while its application to equities is limited due to the large size of the investable sets and to the corresponding elaborate risk models (see, for instance, [34], [35] and [36]).

From a modelling point of view, we contribute to the literature by proposing a novel equity portfolio design that aims at overcoming these difficulties with the introduction into the classical mean-variance framework of both a cardinality constraint and a risk parity condition. The first is used to limit the number of assets in the portfolio, while the second properly controls the distribution of risks among its constituents. The resulting risk parity based cardinality constrained portfolio optimization problem will be denoted by RP-CCPOP. From a computational point of view, we develop a variant of the multi-objective particle swarm optimization (MOPSO) algorithm proposed by [37]. In our algorithm, candidate

solutions are represented by a pair of vectors. The first of them includes portfolio weights, while the second conveys possible rebalancing information, that will be used to modify the first vector according to the paradigms of particle swarm optimization. Further, a swap mutation operator has been added to increase exploration capabilities. The implementation of a novel scheme to handle at the same time cardinality, buy-in thresholds, budget and risk parity constraints is also considered. This procedure combines a repair mechanism for the first three constraints with a domination principle to compare solutions in terms of deviations from risk parity. Three alternatives are taken into account to this end, namely the constrained domination principle by [38], a self-adaptive tolerance method similar to the one developed by [39] and the self-adaptive penalty technique presented in [40]. Once a constraint-handling method is selected from these alternatives, the resulting hybrid constraint-handling multi-objective particle swarm optimization algorithm will be generally denoted by HMOPSO. Table 1 points out the contributions of the proposed algorithm with respect to some popular PSO variants adopted in the portfolio optimization field.

The rest of the paper is organized as follows. In Section 2, we formally describe the equity portfolio optimization problem, and discuss different implementations of the risk parity principle. Section 3 reports the description of the developed multi-objective evolutionary optimization algorithm with its three variants of the constraint-handling technique. Section 4 is devoted to the discussion and assessment of the proposed algorithms on a set of real-world experiments. The best alternative is then used to validate the novel portfolio investment strategy with respect to the standard cardinality constrained portfolio optimization model in an out-of-sample setting. Finally, the concluding remarks are presented in Section 5.

## 2. Problem formulation

### *2.1. Cardinality constrained portfolio optimization*

Consider a financial market consisting of $n$ risky assets modeled through a probability space. A portfolio is represented by a weight vector $\mathbf{x} = (x_1, \ldots, x_n)^\top$, where $x_i \in \mathbb{R}$ denotes the proportion of capital invested in asset $i$. Assume that agents act their decisions over a one-period horizon and the random rate of return of asset $i$ at the end of the investment period, denoted as $R_i$, has a continuous probability density function (pdf), then the rate of return of a portfolio $\mathbf{x}$ is the random variable

$$R(\mathbf{x}) = \sum_{i=1}^{n} x_i R_i \tag{1}$$

having the pdf $f_{R(\mathbf{x})}$ induced by that of $(R_1, \ldots, R_n)^\top$. $R(\mathbf{x})$ is measurable in $(R_1, \ldots, R_n)$ with expected value

$$\mu_p(\mathbf{x}) = \mathbb{E}(R(\mathbf{x})) = \mathbf{x}^\top \mu \tag{2}$$

and variance given by

$$\sigma_p^2(\mathbf{x}) = \mathbf{x}^\top C \mathbf{x} \tag{3}$$

| Algorithm | Portfolio model | Methodology | Contribution |
|---|---|---|---|
| PSO [12] | CCPOP | SO | the hybrid solution representation by [41] is used for the particles; PSO and discrete PSO are integrated; a repair mechanism handles contraints |
| VC-HPSO [42] | CCPOP | SO | particle velocity is clamped; a mutation operator is added and parameters are adaptively updated |
| NS-MOPSO [43] | CCPOP | MO | the hybrid solution representation by [41] is used for the particles; the non-dominated sorting is adapted to satisfy both the objectives and the constraints; velocity is clamped and its direction changes with a fixed probability |
| DMS-MOPSO [44] | mean-variance with no-short selling | MO | solutions are represented by real vectors; the non-dominated sorting is adapted to satisfy both the objectives and the constraints; a set of small sized swarms and a self-learning strategy are used |
| HMOPSO | CCPOP and RP-CCPOP | MO | solutions are represented by real vectors; the non-dominated sorting is adapted to satisfy the objectives; velocity is clamped and its direction changes with a fixed probability; a swap mutation operator is added for obtaining more efficient solutions; three hybrid mechanisms are added to handle constraints |

Table 1: Particle swarm optimization algorithms adopted for solving portfolio optimization problems with cardinality constraints and risk parity. In the third column, SO and MO indicate single-objective and multi-objective optimization, respectively.

where $\mathbb{E}(\cdot)$ denotes the expectation, $\mu = (\mu_1, \ldots, \mu_n)^\top$ and $C$ are the vector of expected values and the covariance matrix of the rates of return of the risky assets, respectively.

According to the modern portfolio theory [1], investors' decisions are based on the first two moments of the rate of return distribution of portfolios. The preference relation is thus the following

**Definition 1.** *Let $\mathcal{X} \subseteq \mathbb{R}^n$ and $\mathbf{x}, \mathbf{y} \in \mathcal{X}$. Then $\mathbf{x}$ (Pareto) dominates $\mathbf{y}$ with respect to $\mathcal{X}$, in symbols $\mathbf{x} \prec \mathbf{y}$, if and only if $\mu_p(\mathbf{x}) \geq \mu_p(\mathbf{y})$ and $\sigma_p^2(\mathbf{x}) \leq \sigma_p^2(\mathbf{y})$ with at least one strict inequality.*

The asset allocation problem reduces to a bi-objective optimization problem where portfolio expected return (2) is maximized and portfolio variance (3) is minimized. Thus, a portfolio $\mathbf{x}^* \in \mathcal{X}$ is (Pareto) optimal if and only if it is non-dominated with respect to $\mathcal{X}$, i.e. there does not exist another portfolio $\mathbf{x} \in \mathcal{X}$ that dominates $\mathbf{x}^*$. The subset of non-dominated portfolios in $\mathcal{X}$ represents the so-called Pareto set. Its image in the mean-variance space is called efficient frontier, or Pareto front.

The starting point of our portfolio design is the model developed by [9], which extends the standard mean-variance formulation by adding a cardinality constraint to control the number of active positions, i.e. assets with positive weight, taken in the portfolio and the corresponding costs.
Assuming each asset weight lies between a lower bound $l_i$ and an upper bound $u_i$, with $0 < l_i < u_i \leq 1$, $i = 1, \ldots, n$, the resulting mixed-integer bi-objective optimization problem can be written as

$$\begin{aligned}
&\text{minimize} && \big(-\mu_p(\mathbf{x}),\ \sigma_p^2(\mathbf{x})\big) && (4)\\
&\text{subject to} && \sum_{i=1}^{n} x_i = 1 && (5)\\
& && \sum_{i=1}^{n} \delta_i = K && (6)\\
& && \delta_i \in \{0,1\} \quad i = 1, \ldots, n && (7)\\
& && \delta_i l_i \leq x_i \leq \delta_i u_i \quad i = 1, \ldots, n. && (8)
\end{aligned}$$

Eq. (5) represents the budget constraint and ensures that all the capital is invested in the portfolio. The cardinality constraint given in (6) imposes that exactly $K$ active positions from the $n$ assets present in the investible universe are selected. Note that $K$ is a parameter decided by the decision-maker. The binary variables $\delta_i$ in (7), $i = 1, \ldots, n$, are employed to model the inclusion or exclusion of asset $i$ in the portfolio and have the following meaning

$$\delta_i = \begin{cases} 0, & \text{if asset } i \text{ is not included in the portfolio} \\ 1, & \text{if asset } i \text{ is included in the portfolio.} \end{cases} \quad (9)$$

Constraint (8) ensures that, if asset $i$ is in the portfolio, i.e. $\delta_i = 1$, its proportion $x_i$ lies between $l_i$ and $u_i$. In the case the asset is not included in the portfolio, i.e. $\delta_i = 0$, constraint (8) imposes the corresponding weight $x_i$ to be 0. Floor constraints, related to $l_i$, are used to control costs while ceiling constraints, related to $u_i$, prevent portfolios from excessive concentration on a singular asset. Note that the assumption $l_i > 0$ imposes no-shortselling.

From now on, the cardinality constrained portfolio optimization problem (4)–(8) will be denoted by CCPOP.

### *2.2. Risk-parity portfolios*

CCPOP simultaneously manages profit and risk [45]. However, this approach may be unsuitable for investors having reduction of large losses and diversification across sources of risk as primary goals. An allocation strategy solely relying on risk views to manage risk may be advisable in this case [34].
The level of diversification within a portfolio can be measured by the distribution of risk contributions of its constituents [3]. By representing the risk of a portfolio as the volatility of its rates of return, i.e. $\sigma_p(\mathbf{x}) = \sqrt{\mathbf{x}^\top C \mathbf{x}}$, we have

the following risk decomposition

$$\sigma_p(\mathbf{x}) = \sum_{i=1}^{n} x_i \frac{\partial \sigma_p(\mathbf{x})}{\partial x_i} = \sum_{i=1}^{n} x_i \left( \frac{Cx}{\sqrt{\mathbf{x}^\top C \mathbf{x}}} \right)_i = \sum_{i=1}^{n} x_i \frac{(Cx)_i}{\sqrt{\mathbf{x}^\top C \mathbf{x}}} \tag{10}$$

where $(Cx)_i$ is the $i$-th component of the vector $Cx$. Denote the risk contribution from asset $i$ by $\mathrm{RC_i}(\mathbf{x}) = x_i \dfrac{\partial \sigma_p(\mathbf{x})}{\partial x_i}$, and define the corresponding relative risk contribution as

$$\mathrm{RRC}_i(\mathbf{x}) = \frac{\mathrm{RC_i}(\mathbf{x})}{\sigma_p(\mathbf{x})} = \frac{x_i (Cx)_i}{\sigma_p^2(\mathbf{x})}. \tag{11}$$

The paper will focus on the following risk control strategy known as risk parity [20].

**Definition 2.** *Let $C$ be a positive definite covariance matrix of order $n$, a portfolio $\mathbf{x} \in \mathcal{X}$ with $K$ active positions is called a risk parity (RP) portfolio with respect to $C$ if it satisfies the condition*

$$\mathrm{RC}_i(\mathbf{x}) = \frac{\sigma_p(\mathbf{x})}{K} \tag{12}$$

*for all $i$ such that $\delta_i = 1$, where $\delta_i$ is given in (9).*

An RP portfolio is thus characterized by the requirement of having equal risk contributions from each active asset. Based on (11), a portfolio $\mathbf{x} \in \mathcal{X}$ attains risk parity if and only if $\mathrm{RRC}_i(\mathbf{x}) = 1/K$, for all $i$ such that $\delta_i = 1$.

This type of portfolio presents appealing properties for diversification purposes, as reported in [23]. However, existence and uniqueness of a solution satisfying (12) are only guaranteed in the full invested and long-only setting [46]. Thus, using numerical methods becomes fundamental to solve RP portfolio selection problems with more complex constraints.

The problem of identifying an RP portfolio in a feasible set $\mathcal{X}$ can be rewritten as an optimization problem with a cost function quantifying the deviation from risk parity. A first example of such a function considers all pairwise differences in squared among the active assets as follows

$$f_1^{RP}(\mathbf{x}) = \sum_{i=1}^{n} \sum_{j=1}^{n} \delta_i \delta_j \left( x_i (Cx)_i - x_j (Cx)_j \right)^2. \tag{13}$$

One can alternatively measure deviations of RRCs from the average value in squared or absolute sense, obtaining the following cost functions

$$f_2^{RP}(\mathbf{x}) = \sum_{i=1}^{n} \delta_i \left( \frac{x_i (C\mathbf{x})_i}{\mathbf{x}^\top C \mathbf{x}} - \frac{1}{K} \right)^2 \tag{14}$$

and

$$f_3^{RP}(\mathbf{x}) = \sum_{i=1}^{n} \delta_i \left| \frac{x_i (C\mathbf{x})_i}{\mathbf{x}^\top C \mathbf{x}} - \frac{1}{K} \right| \tag{15}$$

respectively. In all the proposed cases, portfolios with cost function value equal to zero achieve risk parity.

Due to the non-smoothness and non-convexity of $f_1^{RP}$, $f_2^{RP}$ and $f_3^{RP}$, approximation and heuristic approaches are used to solve the corresponding minimization problems (see, for instance, [29] and [32]).

### *2.3. Reconciling profit with risk control*

In this paper, we propose to manage performance and risk dimensions at the same time by integrating the RP condition (12) into CCPOP. The resulting portfolio optimization problem, which will be denoted by RP-CCPOP, can be formulated as follows

$$\text{minimize} \quad \left(-\mathbf{x}^\top \mu,\ \mathbf{x}^\top C\mathbf{x}\right) \tag{16}$$

$$\text{subject to} \quad \sum_{i=1}^{n} x_i = 1 \tag{17}$$

$$\sum_{i=1}^{n} \delta_i = K \tag{18}$$

$$\delta_i \in \{0,1\} \quad i = 1,\ldots,n \tag{19}$$

$$\delta_i l_i \leq x_i \leq \delta_i u_i \quad i = 1,\ldots,n. \tag{20}$$

$$x_i \left(C\mathbf{x}\right)_i = \delta_i \frac{\mathbf{x}^\top C\mathbf{x}}{K} \quad i = 1,\ldots,n \tag{21}$$

where $0 < l_i < u_i \leq 1$, for $i = 1,\ldots,n$, and the equality constraint (21) represents the risk parity condition.

## 3. Constrained multi-objective particle swarm optimization

Particle swarm optimization (PSO) is a distributed behavioral algorithm that performs multidimensional search by mimicking the movements of a bird flock or a fish schooling that searches for food [47]. The PSO mechanism is based on the communication of information about good solutions through the swarm. In this manner, the particles will tend to move toward good areas in the search space.

The adaptation of this paradigm to deal with portfolio management problems has proved to be very effective (see, for instance, [48] and the references therein for a survey on the subject). In particular, the promising results in the solution of CCPOP obtained by [43] justify our development of a new version of the multi-objective particle swarm optimization (MOPSO) algorithm to handle cardinality, quantity and risk parity constraints at the same time.

### *3.1. Multi-objective particle swarm portfolio optimization*

The algorithm that we propose operates on a set of $S$ candidate solutions, denoted as $\mathcal{P}$. At each iteration $t$, the $s$-th candidate solution is formed by a

pair of $n$-dimensional real vectors $(\mathbf{x}_s(t), \mathbf{v}_s(t))$, for $s = 1, \ldots, S$, where $\mathbf{x}_s(t) = (x_{s1}(t), \ldots, x_{sn}(t))^\top$ gathers the weights of the $s$-th portfolio to be optimized and $\mathbf{v}_s(t) = (v_{s1}(t), \ldots, v_{sn}(t))^\top$ is an update vector conveying the information about possible rebalancing of $\mathbf{x}_s$. The set of decision variables $\delta_i$, $i = 1, \ldots, n$, in Problem (16)–(21) are implicitly handled as follows: for each weight vector $\mathbf{x}_s(t)$, the $K$ assets with the highest weights enter the corresponding portfolio while zero weight is assigned to the remaining $n - K$ assets. In this manner, the cardinality constraint is implicitly satisfied while the assumption $l_i > 0$ for all $i = 1, \ldots, n$ avoids the indecisiveness case represented by $\delta_i = 1$ and $x_i = 0$.

Using a Pareto ranking scheme based on Definition 1, there are two types of promising solutions that play a part in determining $\mathbf{v}_s(t)$: from one hand, the most recent non-dominated portfolio $\mathbf{x}_s^{best}$ related to candidate solution $s$ and, from the other hand, all the non-dominated portfolios found along the optimization process. We denote this second set as $\mathcal{G}^{best}$ and fix its maximal size to $S$. Following the procedure stated in [37], if the number of elements of $\mathcal{G}^{best}$ exceeds $S$, some portfolios are pruned as follows: first, an adaptive grid divides the mean-variance space into a number $div$ of squares, then the most densely populated squares are truncated. At this point, a fitness value is assigned to each square that contains members of $\mathcal{G}^{best}$ equal to the result of dividing any number $\gamma > 1$ by the number of resident portfolios. Thus, a more densely populated square is given a lower score. A roulette wheel selection of a square in the objective space according to its score is performed and a member $\mathbf{g}_s^{best}$ of that square is randomly chosen. The update rule for $\mathbf{v}_s$ becomes

$$\mathbf{v}_s(t+1) = w\mathbf{v}_s(t) + c_1 rand_1(\mathbf{x}_s^{best} - \mathbf{x}_s(t)) + c_2 rand_2(\mathbf{g}_s^{best} - \mathbf{x}_s(t)) \quad (22)$$

for $s = 1, \ldots, S$. The term $w\mathbf{v}_s(t)$, called in literature momentum, regulates the importance of $\mathbf{v}_s(t)$ in $\mathbf{v}_s(t+1)$ through the inertia weight $w$. The second term, called cognitive component, quantifies how much displacement, starting at $\mathbf{x}_s(t)$, is needed to reach the corresponding non-dominated portfolio $\mathbf{x}_s^{best}$. The social component is represented by the third addend and quantifies the performance of portfolio $s$ relative to the best portfolio selected in $\mathcal{G}^{best}$. Higher values for $w$ result in a good global search characteristic, while lower values produce a refined localized search. Parameters $c_1$ and $c_2$ are positive acceleration coefficients used to weight the contribution of cognitive and social components respectively, while $rand_1$ and $rand_2$ represent two random numbers generated by a uniform distribution on the interval $[0, 1]$.

The portfolio composition of the $s$-th candidate solution can now be modified according to the following formula

$$\mathbf{x}_s(t+1) = \mathbf{x}_s(t) + \mathbf{v}_s(t+1) \quad (23)$$

for $s = 1, \ldots, S$.

All the weight vectors $\mathbf{x}_s^{best}$ and the external archive $\mathcal{G}_{best}$ are updated after every iteration.

*3.2. Solution clamping and mutation*

Since large weight updates may cause portfolios to leave the domain boundaries, we consider the following clamping procedure proposed by [49] to control the portfolio rebalancing components

$$v_{si}(t) = \begin{cases} v_i^{\min}, & \text{if } v_{si}(t) < v_i^{\min} \\ v_i^{\max}, & \text{if } v_{si}(t) > v_i^{\max} \\ v_{si}(t), & \text{otherwise} \end{cases} \tag{24}$$

for $s = 1, \ldots, S$ and $i = 1, \ldots, n$, where $v_i^{\min}$ and $v_i^{\max}$ are minimum and maximum percentage of capital that are allowed to be moved for asset $i$ respectively.

In order to promote diversity and higher explorative capability, we assign to $v_{si}(t)$ a probability $p_{m_1}$ of being specified in a different direction as in [43]. Moreover, a swap mutation operator is applied to each portfolio $\mathbf{x}_s(t)$ in order to explore un-reached areas of the search space. The operator swaps the weights of two constituents in every candidate solution with a probability $p_{m_2}$ as follows. Let $\mathbf{x} \in \mathcal{X}$ be a portfolio subject to swap mutation and $a$ and $b$ be two randomly chosen positions such that $x_a = 0$ and $l_b \leq x_b \leq u_b$ then the mutated $\mathbf{x}$ is defined componentwise as

$$\tilde{x}_i = \begin{cases} x_i, & \text{if } i \neq a \text{ and } i \neq b \\ l_a + \dfrac{x_b - l_b}{u_b - l_b}(u_a - l_a), & \text{if } i = a \\ 0, & \text{if } i = b. \end{cases} \tag{25}$$

The new candidate solution $\tilde{\mathbf{x}}$ maintains $K$ active positions and satisfies quantity constraints for $a$ and removes asset $b$ from the portfolio.

*3.3. Candidate solutions initialization and constraint-handling techniques*

The set of candidate solutions is initialized randomly with assets positions uniformly distributed between their respective bounds $l_i$ and $u_i$. By applying the proposed selection method, we obtain a set of particles that satisfy cardinality, floor and ceiling constraints. The repair transformations reported below deal with the full investment condition.

**Proposition 1** ([50])**.** *Let* $\mathbf{x} \in \mathbb{R}^n$ *and* $I_+ = \{i = 1, \ldots, n \mid x_i > 0\}$, $|I_+| = K$, *and assume*

1. $l_i \leq x_i \leq u_i$ *for all* $i \in I_+$,
2. $\sum_{i \in I_+} l_i < 1$,
3. $\sum_{i \in I_+} u_i > 1$.

*Then, the portfolio* $\tilde{\mathbf{x}} = (\tilde{x}_1, \ldots, \tilde{x}_n)^\top$ *defined as* $\tilde{x}_i = 0$ *for* $i \notin I_+$, *and, for all* $i \in I_+$,

$$\tilde{x}_i = \begin{cases} u_i - \dfrac{(u_i - x_i)}{\sum_{j \in I_+}(u_j - x_j)} \left( \sum_{j \in I_+} u_j - 1 \right), & \text{if } \sum_{j \in I_+} x_j < 1 \\ x_i, & \text{if } \sum_{j \in I_+} x_j = 1 \\ l_i + \dfrac{(x_i - l_i)}{\sum_{j \in I_+}(x_j - l_j)} \left( 1 - \sum_{j \in I_+} l_j \right), & \text{if } \sum_{j \in I_+} x_j > 1 \end{cases} \tag{26}$$

*preserves the invested positions of* $\mathbf{x}$*, satisfies the constraints* $l_i \leq \tilde{x}_i \leq u_i$*, for all* $i \in I_+$*, and* $\sum_{j=1}^{n} \tilde{x}_j = 1$.

This update rule does not modify portfolio constituents and involves proportionate distribution of allocation over non-zero assets in order to follow the required budget, floor and ceiling constraints.

The risk parity equality constraints in (21) are dealt with by applying a suitable constraint-handling technique based on the Pareto dominance principle. In particular, we will analyze the hybridization capabilities of the following procedures with the repair mechanism (26):

1. the constrained-domination principle proposed in [38];
2. the constrained method developed in [39];
3. the self-adaptive penalty technique presented in [40].

Before introducing the characteristics of these constraint-handling methods, we transform (21) into inequality constraints as follows

$$\left| x_i \left(C\mathbf{x}\right)_i - \delta_i \frac{\mathbf{x}^\top C\mathbf{x}}{K} \right| \leq \tau, \quad i = 1, \ldots, n \tag{27}$$

where $\tau \geq 0$ is a tolerance parameter according to which infeasible solutions close to the feasible region are retained in order to improve the search effectiveness. The violation of constraint $i$ in (21) for an individual $\mathbf{x}$ can be measured as

$$c_i(\mathbf{x}, \tau) = \max \left\{ \left| x_i \left(C\mathbf{x}\right)_i - \delta_i \frac{\mathbf{x}^\top C\mathbf{x}}{K} \right| - \tau, 0 \right\}, \quad i = 1, \ldots, n. \tag{28}$$

Let $c_i^{max}$ denote the maximum of $c_i(\mathbf{x}, \tau)$ over all portfolios in the current iteration and define

$$\phi_i(\mathbf{x}, \tau) = \begin{cases} \dfrac{c_i(\mathbf{x}, \tau)}{c_i^{max}}, & \text{if } c_i^{max} > 0 \\ 0, & \text{otherwise} \end{cases} \tag{29}$$

for $i = 1, \ldots, n$, the overall constraint violation can be expressed as

$$\phi(\mathbf{x}, \tau) = \frac{1}{n} \sum_{i=1}^{n} \phi_i(\mathbf{x}, \tau). \tag{30}$$

Note that $c_i^{max}$ varies during the evolution in order to balance the contribution of each constraint in the problem irrespective of their differing ranges.

*3.3.1. Constrained domination principle*

The constrained-domination principle, shortly CDP, compares pairwise solutions according to the following three feasibility criteria:

i) when two feasible portfolios are compared, the one Pareto dominating the other is chosen;

ii) when a feasible portfolio is compared with an infeasible portfolio, the feasible one is chosen;

iii) when two infeasible portfolios are compared, the one with the lowest overall constraint violation is chosen.

Therefore, the CDP always considers feasible solutions better than infeasible ones. When two feasible solutions are considered, they are only compared in terms of their objective function values since the corresponding overall constraint violations are zero. In the case of two infeasible solutions, the comparison is based on the sum of constraints violations. This rule aims at pushing infeasible individuals to the feasible region.

*3.3.2. Self-adaptive tolerance constrained domination method*

Our variant of the self-adaptive tolerance constrained method proposed in [39] first exploits the projection mechanism of Proposition 1 for the budgeting and quantity constraints and then adaptively relaxes the risk parity constraint (21) according to Eqns. (28)–(30), with $\tau$ changing over time as follows

$$\tau(t) = \begin{cases} \text{median}\left\{\phi(\mathbf{x}_s(t), 0) \mid s = 1, \ldots, S\right\}, & \text{if } t = 0 \\ \tau(t-1)\left(1 - r_f(t)\right), & \text{otherwise} \end{cases} \tag{31}$$

where $r_f(t)$ denotes the feasibility ratio of the portfolios at iteration $t$, i.e. the ratio of the number of feasible portfolios at time $t$ to the size $S$ of the set $\mathcal{P}$. Since the extent of relaxation depends on the feasibility of the elements in $\mathcal{P}$, when fewer portfolios are feasible, the rate of reducing $\tau$ will be slower. Hence, more generations will be required to find feasible solutions. For example, when all individuals in the current set are infeasible, $\tau$ will not be reduced until some feasible portfolios are found.

By incorporating this adaptive relaxation of constraints into the CDP approach, the method provides a dynamic sorting that depends on the number of risk parity deviations in $\mathcal{P}$. More specifically, we have the following

**Definition 3.** *Let* $\mathbf{x}$, $\mathbf{y}$ *be two portfolios satisfying* (17)–(20) *and* $\tau$ *be defined as in* (31)*, then we say that* $\mathbf{x}$ $\tau$*-dominates* $\mathbf{y}$ *and write* $\mathbf{x} \prec_\tau \mathbf{y}$ *if and only if*

$$\begin{cases} \mathbf{x} \prec \mathbf{y}, & \text{if } \phi(\mathbf{x}, 0) \leq \tau(t) \text{ and } \phi(\mathbf{y}, 0) \leq \tau(t) \\ \mathbf{x} \prec \mathbf{y}, & \text{if } \phi(\mathbf{x}, 0) = \phi(\mathbf{y}, 0) \\ \phi(\mathbf{x}, 0) < \phi(\mathbf{y}, 0), & \text{otherwise} \end{cases} \tag{32}$$

*where* $\mathbf{x} \prec \mathbf{y}$ *denotes Pareto dominance as stated in Definition 1 and* $\tau(t)$ *is the tolerance level at time* $t$*.*

This ordering compares two solutions using only their objective function values if both solutions are feasible, slightly feasible (as determined by the value of $\tau$) or even if they have the same sum of constraint violations. Conversely, if both solutions are infeasible, they are compared based on only their overall constraint violations. In the extreme case in which $r_f(t) = 1$, (32) reduces to the CDP feasibility rules in that generation.

*3.3.3. Self-adaptive penalty constrained domination method*

Similar to the method just described, the self-adaptive penalty technique uses the information gathered from the search process to control the amount of penalty added to infeasible individuals. More specifically, two types of penalty are added to each infeasible individual to identify the best infeasible individuals in the current population. The amount of the added penalties depends on the number of feasible individuals present in the current population. On the one hand, if there is a small proportion of feasible individuals, then infeasible individuals with a higher amount of constraint violation will have a higher amount of penalty. On the other hand, if there is a large number of feasible individuals, then small penalties will be added to infeasible individuals with high fitness values. These two penalties will allow the algorithm to switch between finding more solutions that are feasible and searching for optimal solutions at any time during the search process.

The procedure involves the following computations. First, the values of the two objective functions, namely $\mu_p$ and $\sigma_p^2$, of each candidate portfolio $\mathbf{x}_s$ in $\mathcal{P}$ are normalized using the formulas

$$f_1(\mathbf{x}_s) = \frac{\max\limits_{s'} \mu_p(\mathbf{x}_{s'}) - \mu_p(\mathbf{x}_s)}{\max\limits_{s'} \mu_p(\mathbf{x}_{s'}) - \min\limits_{s'} \mu_p(\mathbf{x}_{s'}) + \epsilon} \tag{33}$$

and

$$f_2(\mathbf{x}_s) = \frac{\sigma_p^2(\mathbf{x}_s) - \min\limits_{s'} \sigma_p^2(\mathbf{x}_{s'})}{\max\limits_{s'} \sigma_p^2(\mathbf{x}_{s'}) - \min\limits_{s'} \sigma_p^2(\mathbf{x}_{s'}) + \epsilon} \tag{34}$$

where $\epsilon$ is a positive value for preventing the denominators from becoming zero in the case $\min\limits_{s'} \mu_p(\mathbf{x}_{s'}) = \max\limits_{s'} \mu_p(\mathbf{x}_{s'})$ or $\min\limits_{s'} \sigma_p^2(\mathbf{x}_{s'}) = \max\limits_{s'} \sigma_p^2(\mathbf{x}_{s'})$. We have set $\epsilon = 10^{-6}$ in the numerical analysis as [51]. These scaling functions map the original objective space $\mathbb{R}^2$ to $[0, 1]^2$.

The overall constraint violation of the risk parity is then calculated according to Eqns. (28)–(30).

Depending on the feasibility ratio $r_f$, the final value of the $j$-th modified objective function for $\mathbf{x}_s$ is defined as

$$F_j(\mathbf{x}_s) = \begin{cases} \phi(\mathbf{x}_s, \tau), & \text{if } r_f = 0 \\ \sqrt{f_j(\mathbf{x}_s)^2 + \phi(\mathbf{x}_s, \tau)^2} + (1 - r_f)\phi(\mathbf{x}_s, \tau) + r_f f_j(\mathbf{x}_s), & \text{if } r_f \neq 0 \text{ and } \mathbf{x}_s \notin \mathcal{X} \\ f_j(\mathbf{x}_s), & \text{if } r_f \neq 0 \text{ and } \mathbf{x}_s \in \mathcal{X} \end{cases} \tag{35}$$

with $j = 1, 2$. The population can now be sorted by CDP based on $F_1$ and $F_2$.

The pseudocode of HMOPSO is outlined in Algorithm 1, where $CHT$ indicates the variant of the hybrid operator that is implemented.

## 4. Performance metrics

Several criteria are considered to assess the quality of the proposed HMOPSO and the profitability of the designed portfolio optimization model.

**Algorithm 1:** HMOPSO for RP-CCPOP

**Input** : $\mathbf{l}$, $\mathbf{u}$, $t_{max}$, $S$, $c_1$, $c_2$, $w$, $p_{m_1}$, $p_{m_2}$, $div$, $\gamma$, $\mathbf{v}^{min}$, $\mathbf{v}^{max}$, $\tau$, $CHT$
**Output**: $\mathcal{G}_{\text{best}}$

Randomly generate a set of portfolios $\mathbf{x_s}(0)$, $s = 1, \ldots, S$
Set the corresponding rebalancing vectors $\mathbf{v}_s(0) = 0$
Set $\mathcal{P} = \{(\mathbf{x_s}(0), \mathbf{v}_s(0)) : s = 1, \ldots, S\}$
Modify each member of $\mathcal{P}$ using (26) and evaluate its overall constraint violation for the risk parity constraint using (28)–(30)
Initialize $\mathbf{x}_s^{best} = \mathbf{x_s}(0)$, $s = 1, \ldots, S$
Initialize $\mathcal{G}^{best}$ based on $CHT$
Let $t = 0$
**while** $t \leq t_{max}$ **do**
    **for** $s = 1$ *to* $S$ **do**
        Select $\mathbf{g}_s^{best} \in \mathcal{G}^{best}$ on the basis of $CHT$
        Update $\mathbf{x}_s^{best}$ on the basis of $CHT$ and $\mathbf{x_s}(t)$
    **end**
    $t = t + 1$
    Update $\mathbf{v}_s(t)$ using (22) and adjust it through (24)
    **for** $i = 1$ *to* $n$ **do**
        **if** $rand < p_{m_1}$ **then**
            $\mathbf{v}_{si}(t) = -\mathbf{v}_{si}(t)$
        **end**
    **end**
    Update $\mathcal{P}$ using (23)
    Modify $\mathcal{P}$ using (26)
    Mutate $\mathcal{P}$ using (25)
    Evaluate $\mathcal{P}$ according to $CHT$
    Update $\mathcal{G}^{best}$ according to $CHT$
**end**

### *4.1. In-sample performance metrics*

According to the prescriptions in [52], multiple runs are employed in order to obtain a sample of competing fronts for each algorithm and for each instance of the test problems.

Since the true Pareto fronts are unknown, the effectiveness of each procedure has been measured on the basis of three criteria:

i) the diversification level attained by the optimal portfolios;
ii) the capacity to generate an appropriate number of non-dominated solutions that satisfy the risk parity principle at least approximately;
iii) the capacity of the approximated Pareto front to converge toward the true Pareto front by spanning a suitable portion of non-dominated risk-return profiles.

Accordingly, optimal solution sets with large number of well-diversified feasible non-dominated portfolios, enclosing large areas of the risk-return space and scattering evenly are generally desirable.

Two performance metrics are used to summarize the in-sample experimental results. The first indicator is the Herfindahl index of risk contributions [20], defined as

$$h(\mathbf{x}) = \sum_{i=1}^{n} \left( \frac{x_i \left(C\mathbf{x}\right)_i}{\mathbf{x}^\top C\mathbf{x}} \right)^2 . \tag{36}$$

It simultaneously quantifies the magnitude of deviations from risk parity and the diversification level of the portfolio $\mathbf{x} \in \mathcal{X}$. If there are $K$ active positions, then it is easy to verify that $1/K \leq h(\mathbf{x}) \leq 1$. When $h(\mathbf{x}) = 1$, the risk contribution is concentrated in only one asset. For $h(\mathbf{x}) = 1/K$ the portfolio is fully diversified among the active assets, thus satisfying condition (12).

Preliminary to the introduction of the second performance metric, which will be used to compare the overall quality of the approximation sets, is the notion of hypervolume indicator [53]. The hypervolume of a given (approximated) Pareto front $PF$ measures the size of the region of the objective space dominated by at least one of the members of $PF$ and bounded by a selected reference point, that is dominated by all the points of $PF$. In our context, with two objectives to minimize, the reference point is $\mathbf{r} = (r_1, r_2)$ and the hypervolume is computed by

$$HV(PF, \mathbf{r}) = \text{Leb}\left(\cup_{(y_1,y_2)\in PF} \left[y_1, r_1\right] \times \left[y_2, r_2\right]\right) \tag{37}$$

where $\text{Leb}(A)$ is the Lebesgue measure of a set $A$. In this manner, $HV$ evaluates the closeness of the solutions to the optimal set and captures the spread of the solutions over the objective space. Thus, larger hypervolume indicator values imply a larger distance from the reference point and indicate solutions are scattered more evenly in the objective space.

Despite its effectiveness in evaluating an approximation, the hypervolume indicator presents some drawbacks. From one hand, it is sensitive to the relative scaling of the objectives and to the presence or absence of extremal points in a front ([54] and [55]). This results in favoring an approximation set which has better converged for the least-scaled objective function or has more points that are extremal. On the other hand, hypervolume depends strongly on the choice of the reference point [56]. Different reference points may result in different evaluations. Moreover, all possible vectors in the comparison must dominate the reference point; otherwise, the evaluations of the indicator may not make any sense, for example, reporting negative values [57].

In this study, assuming the approximation sets have cardinality $S \geq 2$, the following procedure is proposed to avoid these pitfalls. First, the objective function values are projected onto the interval $[0, 1]$ by Eqns. (33) and (34). Second, noting that in the $[0, 1]^2$ space the worst solution for our optimization problem is represented by the point $(1, 1)$, we choose as reference point the vector

$$\mathbf{r} = (1 + r, 1 + r) \tag{38}$$

where $r > 0$. In the experiments we will set $r = \sqrt{2}/(S-1)$, adapting [58]. With this choice of $\mathbf{r}$, fronts with uniformly distributed points are preferred. The evaluation of the hypervolume is conducted as follows.

**Proposition 2.** *Let* $\widehat{PF} = \left\{(y_1^s, y_2^s) \in [0,1]^2 \mid s = 1, \ldots, S\right\}$, $S \geq 2$, *be a normalized discrete Pareto front for the RP-CCPOP, then the corresponding hypervolume indicator with respect to the reference point* (38) *can be formulated as*

$$HV\left(\widehat{PF}, \mathbf{r}\right) = \sum_{s=1}^{S-1} \left(y_1^{s+1} - y_1^s\right)\left(1 - y_2^s\right) + \left(1 - y_1^S\right)\left(1 - y_2^S\right) + r(1 - y_1^1) + \\ + r(1 - y_2^S) + r^2. \tag{39}$$

*Proof.* Without loss of generality, let us assume that the solutions in $\widehat{PF}$ are sorted by the first criterion in ascending order, i.e. $y_1^s \leq y_1^{s+1}$, for $s = 1, \ldots, S-1$. The hypervolume indicator with respect to $\mathbf{r} = (1+r, 1+r)$ is then

$$\begin{aligned} HV\left(\widehat{PF}, \mathbf{r}\right) &= \left(y_1^2 - y_1^1\right)\left(1 - y_2^1 + r\right) + \ldots + \left(y_1^S - y_1^{S-1}\right)\left(1 - y_2^{S-1} + r\right) + \\ &\quad + \left(1 - y_1^S + r\right)\left(1 - y_2^S + r\right) \\ &= \sum_{s=1}^{S-1} \left(y_1^{s+1} - y_1^s\right)\left(1 - y_2^s\right) + \left(1 - y_1^S\right)\left(1 - y_2^S\right) + r(1 - y_1^1) + \\ &\quad + r(1 - y_2^S) + r^2. \end{aligned}$$

□

We can now describe the second performance metric used in the experiments, the so-called contribution rate indicator [58]. To this end, let $PF_1$, $PF_2$ and $PF_3$ be the approximation fronts generated by the three versions of HMOPSO and denote by $PF$ their combination based on Pareto dominance definition. Since the true Pareto front is unknown and $PF$ is the best available approximation, $PF$ is regarded as a surrogate for the true Pareto front. The procedure to compute the contribution rate indicator is as follows.

1. From each approximated Pareto front $PF_i$, $i = 1, 2, 3$, obtain the subset $PF_i' = PF_i \cap PF$, i.e. the set of criterion vectors in $PF_i$ which are not dominated by $PF$.
2. Normalize $PF$ and $PF_i'$, $i = 1, 2, 3$, by employing (33) and (34) with $\epsilon = 0$ and using as extreme values those in $PF$. Denote these sets as $\widehat{PF}$ and $\widehat{PF}_i$, $i = 1, 2, 3$, respectively.
3. Calculate the hypervolume indicators $HV\left(\widehat{PF}, \mathbf{r}\right)$ and $HV\left(\widehat{PF}_i, \mathbf{r}\right)$, $i = 1, 2, 3$, with respect to the reference point (38) according to Eq. (39).

4. Define the contribution rate associated to each approximation set as

$$CR\left(\widehat{PF}_i, \widehat{PF}, \mathbf{r}\right) = \frac{HV\left(\widehat{PF}_i, \mathbf{r}\right)}{HV\left(\widehat{PF}, \mathbf{r}\right)}, \quad i = 1, \ldots, n. \tag{40}$$

Values of $CR\left(\widehat{PF}_i, \widehat{PF}, \mathbf{r}\right)$ close to 1 suggest that the $i$-th approximation front is very close to the surrogate Pareto front. Moreover, if $CR\left(\widehat{PF}_i, \widehat{PF}, \mathbf{r}\right) > CR\left(\widehat{PF}_j, \widehat{PF}, \mathbf{r}\right)$, with $i \neq j$, then $PF_i$ is a better approximation than $PF_j$, and the comparison of the contribution rate gives a sense of the magnitude of the difference.

A rigorous assessment of the robustness of the results can then be performed on the basis of nonparametric inference testing. In particular, we use the Wilcoxon's rank-sum test for independent samples at the 5% significance level to judge whether the results obtained with the best performing procedure differ from the results of the rest of competitors in a statistically significant way.

### *4.2. Out-of-sample performance metrics*

We evaluate the out-of-sample performance of each portfolio optimization model with a set of statistics. Let us denote by $t_0$ and $T$ the last in-sample and the last out-of-sample time respectively and let us indicate by $r_t^{out}$, $t = t_0 + 1, \ldots, T$, the portfolio rates of return for each strategy in the out-of-sample period, respectively. The first performance measure we introduce is the Sharpe ratio [59], which evaluates the compensation earned per unit of portfolio total risk. It is defined as the ratio between the annualized average $\mu^{out}$ of $r_t^{out}$, and the annualized sample standard deviation $\sigma^{out}$ as follows

$$SR = \frac{\mu^{out}}{\sigma^{out}}. \tag{41}$$

The attractiveness of the two investment opportunities is also evaluated by the so-called Omega ratio [60], which gauges favorable and unfavourable excess returns with respect to a user-defined threshold. In this paper, the threshold is set to 0 and the resulting measure can be written in the form

$$\Omega = \frac{\sum_{t=t_0+1}^{T} r_t^{out} \mathbf{1}_{\{r_t^{out} > 0\}}}{-\sum_{t=t_0+1}^{T} r_t^{out} \mathbf{1}_{\{r_t^{out} < 0\}}} \tag{42}$$

where, for a logical proposition $q$, $\mathbf{1}_q = 1$ if $q$ is true, and $\mathbf{1}_q = 0$ otherwise. Higher values of $SR$ and $\Omega$ are preferable.

The downside risk is measured by the maximum drawdown, which represents the maximum loss from a peak to a trough, before a new peak is attained. More precisely, let us consider the cumulative out-of-sample portfolio returns, which correspond to the values of wealth after $t$ periods

$$W_t = W_{t-1}(1 + r_t^{out}) \tag{43}$$

with $t = t_0 + 1, \ldots, T$ and $W_{t_0+1} = 1$, then the drawdowns are defined as

$$DD_t = -\frac{W_t - \max_{t_0+1 \leq s \leq t} W_s}{\max_{t_0+1 \leq s \leq t} W_s}.$$

The maximum drawdown, which corresponds to the largest loss achieved over the out-of-sample, is

$$MDD = max_{t_0+1 \leq s \leq t} DD_t. \tag{44}$$

Two other statistics we also consider to provide further information about the left tail of the portfolio return distribution, namely the value-at-risk and the conditional value-at-risk. After sorting out-of-sample portfolio returns in ascending order, i.e. $r^{out}_{(t_0+1)} \leq r^{out}_{(t_0+2)} \leq \ldots r^{out}_{(T)}$, the value-at-risk at the confidence level $\alpha$ can be defined as

$$VaR_\alpha = -r^{out}_{(\lfloor \alpha(T-t_0-1) \rfloor)} \tag{45}$$

where $\alpha \in (0, 1)$. The conditional value-at-risk at the confidence level $\alpha$ can be estimated as

$$CVaR_\alpha = -\frac{\sum_{t=t_0+1}^{T} r^{out}_{(t)} \mathbf{1}_{\left\{r^{out}_{(t)} \leq -VaR_\alpha\right\}}}{\sum_{t=t_0+1}^{T} \mathbf{1}_{\left\{r^{out}_{(t)} \leq -VaR_\alpha\right\}}}. \tag{46}$$

In the experimental comparison we will set $\alpha = 10\%$.

The average of the diversification index introduced by [61] is used to measure the diversification level of optimal portfolios. It is given by

$$DI = \frac{1}{T - t_0} \sum_{t=t_0+1}^{T} \left(1 - \sum_{i=1}^{n} x_{i,t}^2\right) \tag{47}$$

in which $x_{i,t}$ is the portfolio weight of asset $i$ at time $t$. A greater value of $DI$ implies a greater diversification level.

Finally, to get an impression of the transaction costs involved, we calculate the average turnover over the out-of-sample period as defined in [62]

$$turnover = \frac{1}{T - t_0} \sum_{t=t_0+1}^{T} \sum_{i=1}^{n} |x_{i,t+1} - x_{i,t}| \tag{48}$$

in which $x_{i,t}$ is the portfolio weight of asset $i$ at time $t$ and $x_{i,t+1}$ is the portfolio weight after rebalancing. The value of this statistic equals the average weekly amount of buy and sell transactions as a percentage of the portfolio value. Thus, a greater value of *turnover* indicates a more expensive investment strategy.

## 5. Computational analysis

This section is divided into two parts. First, we assess the capabilities of the variants of HMOPSO to generate well-distributed approximations to the Pareto front for the RP-CCPOP. Then, we compare the performance of the portfolios optimized in terms of the CCPOP with and without the risk parity constraint in order to highlight strengths and weaknesses of the proposed investment strategy.

### 5.1. Comparison of HMOPSO variants

The behavior of the aforementioned variants of HMOPSO is analyzed on the public data sets available in [63]. Specifically, the following three groups of stocks are considered: Dow Jones Industrial Average, Fama and French 49 Industry and NASDAQ 100. Columns 2 to 4 of Table 2 report the periods involved in the experiments with the corresponding number of weeks and assets. In order to analyze robustness and scaling of HMOPSO, and to identify the best choice among the proposed hybrid constraint-handling techniques, we have considered 12 instances of the RP-CCPOP by varying the number $K$ of assets to include in the optimal portfolios according to the dimension $n$ of the investible universe. The last column of Table 2 presents the cardinalities chosen.

| Data set name | Time window | Weeks | Assets ($n$) | Cardinality ($K$) | | | |
|---|---|---|---|---|---|---|---|
| DowJones | 02/1990 – 04/2016 | 1363 | 28 | 5 | 10 | 15 | 20 |
| FF49Industries | 07/1969 – 07/2015 | 2325 | 49 | 5 | 10 | 20 | 40 |
| NASDAQ100 | 11/2004 – 04/2016 | 596 | 82 | 5 | 10 | 20 | 40 |

Table 2: Data sets from [63] with corresponding time window, number of weeks and number of market constituents ($n$) used in the estimation of parameters, and portfolio cardinalities $K$ imposed in each application of HMOPSO.

The expected rates of return and covariance matrices of the stocks are calculated as sample estimates based on all the weekly data available in the corresponding data sets.

The algorithms have been implemented in a MATLAB environment and are run on a PC with Intel Core i7 3.0 GHz with 8 GB RAM.

#### 5.1.1. Parameters setting

Before performing the experiments, HMOPSO parameters have been tuned over the Dow Jones market following the procedure in [64]. The best values are listed in Table 3. Moreover, the tolerance parameter $\tau$ for equality constraints

| Parameter | Value |
|---|---|
| $w$ | 0.4 |
| $c_1$ | 1.494 |
| $c_2$ | 1.494 |
| $v^{\min}$ | 0.002 |
| $v^{\max}$ | 0.2 |
| $p_{m_1}$ | 0.5 |
| $p_{m_2}$ | 0.1 |
| $div$ | 10 |
| $\gamma$ | 10 |
| $S$ | 200 |
| $t_{max}$ | 1000 |

Table 3: Configuration of HMOPSO parameters for the experimental analysis.

relaxation has been fixed to $5 \cdot 10^{-5}$.

For each RP-CCPOP instance, we carried out 20 independent runs of the three versions of HMOPSO to collect statistics. The lower and upper bounds for the stocks weights are $l_i = 0.001$ and $u_i = 1$, $i = 1, \ldots, n$, respectively. These are usual constraint values utilized in the literature (see [16], [50] and [65]). Note that with this choice of bounds, conditions 2 and 3 of Proposition 1 are automatically verified by any combination of assets.

*5.1.2. Experimental results and discussion*

The first analysis focuses on the capability of HMOPSO to generate an appropriate number of feasible non-dominated solutions.
Table 4 reports the mean number of optimal solutions included in the external archive $\mathcal{G}_{best}$, for each variant of the proposed algorithm, and for all instances of RP-CCPOP. Table 5 shows mean and standard deviation values of the Herfindahl index for risk contributions computed as in (36). Table 6 displays the Wilcoxon's rank-sum test for the $h$ values of the optimal portfolios. We can notice that the variants of HMOPSO adopting the constrained domination principle and the self-adaptive tolerance to manage risk parity produce, on average, comparable number of optimal portfolios. Whereas, HMOPSO using the third constraint-handling mechanism generates archives with a size less than a quarter of those of its competitors. It should be noticed that, if we compare the $h$ values of the optimal portfolios identified by the solvers with the corresponding attainable minimum values reported in the second column of Table 5, HMOPSO with self-adaptive penalty provides, on average, the best performance with the lowest standard deviation. The next table confirms the superiority of this variant with respect to that based on the constrained domination principle. The comparison with HMOPSO using self-adaptive tolerance is more complex. The implementation of a self-adaptive penalty outperforms the application of a self-adaptive tolerance in all instances of the Dow Jones data set. However, as the dimension of the market increases, the second mechanism attains better results.

Convergence and diversity are assessed in a single scale through the CR indicator (40). Table 7 displays the corresponding mean and standard deviation values. The results for this metric indicate the use of the constrained domination principle as be the best choice in HMOPSO. The version based on the self-adaptive tolerance presents, in general, slightly worse results. Moreover, the Wilcoxon rank-sum test given in Table 8 corroborates these finding from the statistical point of view.

The mean total CPU times (in seconds) for the examined test problems are listed in Table 9. You can see that the proposed algorithms present similar performance, with a slightly lower computational time for the HMOPSO with self-adaptive penalty.

Summing up, the developed algorithm exploiting the constrained domination principle is able to generate a large number of approximated RP portfolios with satisfactory risk-return tradeoff. The introduction into HMOSPO of a

| data set | $K$ | HMOPSO-CDP | HMOPSO-ST | HMOPSO-SP |
|---|---|---|---|---|
| DowJones | 5 | 199.00 | 198.90 | 58.95 |
| | 10 | 186.20 | 165.75 | 56.45 |
| | 15 | 126.75 | 119.95 | 42.55 |
| | 20 | 100.00 | 101.50 | 25.25 |
| FF49Industries | 5 | 199.95 | 197.90 | 36.00 |
| | 10 | 171.30 | 150.45 | 46.95 |
| | 20 | 86.25 | 77.50 | 21.00 |
| | 40 | 79.65 | 80.85 | 9.70 |
| NASDAQ100 | 5 | 199.10 | 199.55 | 33.50 |
| | 10 | 200.00 | 199.90 | 55.60 |
| | 20 | 162.95 | 145.30 | 34.50 |
| | 40 | 57.80 | 62.50 | 16.15 |

Table 4: Average number of non-dominated solutions included into the external archive $\mathcal{G}_{best}$ of the proposed algorithm adopting the constrained domination principle (HMOPSO-CDP), with self-adaptive tolerance (HMOPSO-ST) and using self-adaptive penalty (HMOPSO-SP) classified by data set and cardinality instance ($K$).

self-adaptive penalty provides the closest results to risk parity, but the sets of efficient portfolios it identifies are very small. In general, the integration of a self-adaptive tolerance to risk parity into HMOPSO guarantees the best balance between the number of optimal solutions produced and the quality of risk parity approximations.

### *5.2. Comparison between CCPOP and RP-CCPOP in terms of Pareto fronts*

In this section, we compare the portfolios obtained by RP-CCPOP with those identified by the cardinality constrained mean-variance model. The comparison is based on the corresponding efficient frontiers.

We obtain a solver for mean-variance problems with cardinality, buy-in thresholds and budget constraints, denoted by HMOPSO$^*$, by removing the mechanism related to the risk parity constraints from HMOPSO. We compare HMOPSO$^*$ with the non-dominated sorting multi-objective particle swarm optimization (NS-MOPSO) algorithm proposed in [43], customized for CCPOP. Similar to HMOPSO$^*$, it bases the exploration of the search space on the non-dominated sorting, uses a repair mechanism for the portfolio constraints, changes velocity direction with a fixed probability and adopts a clamping technique. The main differences are the following. First, NS-MOPSO implements the hybrid solution representation proposed by [41] for defining a portfolio. According to this approach, a binary vector specifies whether a particular asset

| | | | HMOPSO-CDP | | HMOPSO-ST | | HMOPSO-SP | |
|---|---|---|---|---|---|---|---|---|
| data set | $K$ | $h_{min}$ | mean | std | mean | std | mean | std |
| DowJones | 5 | 0.2 | 0.2177 | 0.0427 | 0.2341 | 0.0734 | 0.2081 | 0.0037 |
| | 10 | 0.1 | 0.1203 | 0.0328 | 0.1245 | 0.0429 | 0.1092 | 0.0043 |
| | 15 | 0.0667 | 0.0956 | 0.0332 | 0.0986 | 0.0441 | 0.0758 | 0.0039 |
| | 20 | 0.05 | 0.0889 | 0.0350 | 0.0896 | 0.0391 | 0.0572 | 0.0034 |
| FF49Industries | 5 | 0.2 | 0.2163 | 0.0307 | 0.2150 | 0.0306 | 0.2092 | 0.0045 |
| | 10 | 0.1 | 0.1136 | 0.0187 | 0.1102 | 0.0186 | 0.1078 | 0.0035 |
| | 20 | 0.05 | 0.0682 | 0.0189 | 0.0608 | 0.0168 | 0.0564 | 0.0030 |
| | 40 | 0.025 | 0.0366 | 0.0075 | 0.0358 | 0.0077 | 0.0268 | 0.0015 |
| NASDAQ100 | 5 | 0.2 | 0.2072 | 0.0107 | 0.2140 | 0.0262 | 0.2052 | 0.0027 |
| | 10 | 0.1 | 0.1073 | 0.0067 | 0.1082 | 0.0125 | 0.1068 | 0.0027 |
| | 20 | 0.05 | 0.0580 | 0.0054 | 0.0564 | 0.0049 | 0.0567 | 0.0024 |
| | 40 | 0.025 | 0.0302 | 0.0041 | 0.0287 | 0.0032 | 0.0283 | 0.0013 |

Table 5: Optimal values of Herfindahl index of risk contributions, $h_{min}$, with the corresponding mean and standard deviation values attained by the proposed algorithm adopting the constrained domination principle (HMOPSO-CDP), with self-adaptive tolerance (HMOPSO-ST) and using self-adaptive penalty (HMOPSO-SP) classified by data set and cardinality instance (K).

participates in the portfolio, and a real-valued vector is used to compute the proportions of the budget invested in the assets. Second, it does not consider any mutation operator for the portfolio weights.

The structure of the experiments is the same as that described in Section 5.1, with the data sets and the cardinalities ($K$) listed in Table 2. The parameters used in HMOPSO* are those reported in Table 3. For the NS-MOPSO algorithm, we adopt the parameter setting recommended by [43], i.e. $w = 0.862$, $c_1 = c_2 = 2.05$, $v^{\min} = 0.06$ and $v^{\max} = 0.5$.

It is evident from the computational results given in Table 10, that the proposed simplified version of HMOPSO overperforms its competitor in almost all test problems in terms of contribution rate values. The Wilcoxon's rank-sum test values confirm these findings at a 5% significance level. In particular, we can note that the number of non-dominated solutions identified by HMOPSO* increases with respect to NS-MOSPO as the cardinality $K$ increases.

Based on these results and the consideration made in the previous section, we will adopt the HMOPSO* for the CCPOP strategy while the variant of *HMOPSO* using a self-adaptive tolerance will be used for RP-CCPOP.

Figure 1 displays the approximated Pareto fronts for the CCPOP solutions

| data set | $K$ | HMOPSO-CDP | HMOPSO-ST |
|---|---|---|---|
| DowJones | 5 | $\downarrow$ | $\uparrow$ |
| | 10 | $\uparrow$ | $\uparrow$ |
| | 15 | $\uparrow$ | $\uparrow$ |
| | 20 | $\uparrow$ | $\uparrow$ |
| FF49Industries | 5 | $\leftrightarrow$ | $\downarrow$ |
| | 10 | $\uparrow$ | $\downarrow$ |
| | 20 | $\uparrow$ | $\downarrow$ |
| | 40 | $\uparrow$ | $\uparrow$ |
| NASDAQ100 | 5 | $\uparrow$ | $\uparrow$ |
| | 10 | $\leftrightarrow$ | $\leftrightarrow$ |
| | 20 | $\uparrow$ | $\downarrow$ |
| | 40 | $\uparrow$ | $\downarrow$ |

Table 6: Wilcoxon rank-sum test for the Herfindahl index of risk contributions (36): HMOPSO using self-adaptive penalty (HMOPSO-SP) vs HMOPSO adopting the constrained domination principle (HMOPSO-CDP) and HMOPSO with self-adaptive tolerance (HMOPSO-ST) classified by data set and cardinality ($K$). The symbol "$\uparrow$" means that HMOPSO-SP has yielded better results than the algorithm in the column at a 5% confidence level, "$\downarrow$" indicates that the algorithm in the column is statistically better than HMOPSO-SP and "$\leftrightarrow$" is used when there is no statistical difference between algorithms.

and those of the RP-CCPOP respectively, using the data from the Dow Jones market and varying the cardinality $K$ in $\{5, 10, 15, 20\}$. The RP-CCPOP strategy is able to replicate the CCPOP risk-return profiles for low to medium risks. However, the risk parity condition limits the investment opportunities when allowable risks and cardinality increase. Therefore, for higher levels of risk, RP-CCPOP portfolios have lower profits or even are undefined. This finding is similar to every risk-based strategy.

### *5.3. Out-of-sample comparison of CCPOP and RP-CCPOP strategies*

We now focus on the economic implications of the proposed portfolio optimization model. The magnitude of the potential gains an investor can realize, by using this strategy instead of the CCPOP model, is assessed out-of-sample.

#### *5.3.1. Out-of-sample results and discussion*

The three data sets listed in Table 2 are also used for the out-of-sample analysis. For each of them, we consider the last 53 observations as the test set and readjust optimal portfolio weights at regular calendar intervals, employing the so-called calendar based rebalancing procedure [66]. In particular, two rolling

| | | HMOPSO-CDP | | HMOPSO-ST | | HMOPSO-SP | |
|---|---|---|---|---|---|---|---|
| data set | K | mean | std | mean | std | mean | std |
| DowJones | 5 | 0.8635 | 0.0506 | 0.9916 | 0.0049 | 0.4616 | 0.2104 |
| | 10 | 0.9634 | 0.0144 | 0.9506 | 0.0220 | 0.5480 | 0.0561 |
| | 15 | 0.9644 | 0.0165 | 0.9408 | 0.0165 | 0.4226 | 0.1212 |
| | 20 | 0.9744 | 0.0089 | 0.9445 | 0.0222 | 0.1258 | 0.1614 |
| FF49Industries | 5 | 0.9750 | 0.0119 | 0.9636 | 0.0175 | 0.5824 | 0.0589 |
| | 10 | 0.9823 | 0.0104 | 0.9205 | 0.0334 | 0.5763 | 0.0651 |
| | 20 | 0.9788 | 0.0180 | 0.6527 | 0.2332 | 0.3835 | 0.0824 |
| | 40 | 0.9712 | 0.0175 | 0.9488 | 0.0329 | 0.0748 | 0.1270 |
| NASDAQ100 | 5 | 0.8779 | 0.0867 | 0.9877 | 0.0093 | 0.5048 | 0.2633 |
| | 10 | 0.9559 | 0.0282 | 0.9733 | 0.0218 | 0.3772 | 0.3204 |
| | 20 | 0.9250 | 0.1065 | 0.8526 | 0.0852 | 0.3671 | 0.3115 |
| | 40 | 0.9279 | 0.0756 | 0.7940 | 0.1415 | 0.5391 | 0.1931 |

Table 7: Mean and standard deviation values of the CR performance metric (40) for the proposed algorithm adopting the constrained domination principle (HMOPSO-CDP), with self-adaptive tolerance (HMOPSO-ST) and using self-adaptive penalty (HMOPSO-SP) divided by data set and cardinality ($K$).

window strategies are implemented: one combining 104 weeks to determine optimal portfolios and 1 week for the out-of-sample period, the other using 104 weeks in-sample and 4 weeks out-of-sample. For each in-sample window, the expected rates of return and covariance matrices of the stocks are first calculated as sample estimates, successively HMOPSO* is used to determine CCPOP solutions while the variant of HMOPSO using a self-adaptive tolerance is used for RP-CCPOP portfolios. From each set of non-dominated portfolios, we extract the one which presents the highest in-sample Sharpe ratio. The selected vectors of weights are then kept in the next out-of-sample period for evaluating the corresponding rates of return. The in-sample window is updated by removing the oldest data and including the most recent information, i.e. one week of rates of return in the case of weekly rebalancing and four weeks if the changes are needed monthly. This procedure is repeated until the last available week. Note that the same estimation window is used in both the procedures, since the impact of estimation error in determining optimal portfolios is not under investigation in the paper. In every case, the choice of a 2 years length for the estimation window seems reasonable, since there were no extraordinary economic changes during the period 2013–2016. On the other hand, we test the robustness of the solutions by varying the length of the rebalancing window.

Tables 11, 12 and 13 report the performance statistics of the CCPOP and the

| data set | $K$ | HMOPSO-ST | HMOPSO-SP |
|---|---|---|---|
| DowJones | 5 | ↑ | ↑ |
| | 10 | ↔ | ↑ |
| | 15 | ↑ | ↑ |
| | 20 | ↑ | ↑ |
| FF49Industries | 5 | ↑ | ↑ |
| | 10 | ↑ | ↑ |
| | 20 | ↑ | ↑ |
| | 40 | ↑ | ↑ |
| NASDAQ100 | 5 | ↓ | ↑ |
| | 10 | ↓ | ↑ |
| | 20 | ↑ | ↑ |
| | 40 | ↑ | ↑ |

Table 8: Wilcoxon rank-sum test for the CR performance metric (40): HMOPSO adopting the constrained domination principle (HMOPSO-CDP) vs HMOPSO using self-adaptive tolerance (HMOPSO-ST) and HMOPSO with self-adaptive penalty (HMOPSO-SP) classified by data set and cardinality ($K$). The symbol "↑" means that HMOPSO-CDP has yielded better results than the algorithm in the column at a 5% confidence level, "↓" indicates that the algorithm in the column is statistically better than HMOPSO-CDP and "↔" is used when there is no statistical difference between algorithms.

RP-CCPOP models relative to the first rebalancing procedure for the DowJones, FF49Industries and NASDAQ100 data sets by varying the cardinality $K$. The most profitable strategies in terms of the annualized Sharpe ratio are those implementing RP-CCPOP. However, the quality of the results crucially depends on the choice of the portfolio cardinality. Indeed, for the first two data sets, portfolios with $K \leq 20$ attain the maximum values of $SR$ (1.0302 and 2.0896). In the last experiment, a portfolio with 40 assets guarantees the best performance (0.2433). The CCPOP models involving portfolios with 15 to 40 assets attain the worst results. The two strategies present comparable values for the Omega ratio (42). With respect to the downside risk measures (44), (45) and (46), we can see that the proposed strategy produces the lowest extreme losses. Moreover, the level of diversification of the RP-CCPOP portfolios is slightly better than that attained by the CCPOP portfolios with a lower turnover.

Tables 14, 15 and 16 list the results with monthly rebalancing. For the DowJones data set, the CCPOP portfolios are the most promising in terms of both the Sharpe ratio and the Omega ratio. In the second experiment, the $SR$ criterion indicates the RP-CCPOP with $K = 5$ as the best choice, while $\Omega$ suggests the use of the CCPOP with $K = 5$. For the NASDAQ100, the RP-CCPOP models give the best results of the performance ratios. Overall,

| data set | $K$ | HMOPSO-CDP | HMOPSO-ST | HMOPSO-SP |
|---|---|---|---|---|
| DowJones | 5 | 33.43 | 32.36 | 19.15 |
| | 10 | 43.57 | 44.20 | 32.15 |
| | 15 | 52.89 | 53.41 | 45.26 |
| | 20 | 62.91 | 63.39 | 58.61 |
| FF49Industries | 5 | 43.40 | 45.35 | 32.14 |
| | 10 | 67.69 | 70.10 | 57.91 |
| | 20 | 112.95 | 115.75 | 111.15 |
| | 40 | 214.67 | 218.95 | 215.45 |
| NASDAQ100 | 5 | 67.85 | 68.62 | 55.29 |
| | 10 | 114.49 | 118.31 | 104.98 |
| | 20 | 209.73 | 216.05 | 201.56 |
| | 40 | 404.56 | 406.80 | 396.87 |

Table 9: Mean total CPU times (in seconds) for the proposed algorithm adopting the constrained domination principle (HMOPSO-CDP), with self-adaptive tolerance (HMOPSO-ST) and using self-adaptive penalty (HMOPSO-SP) classified by data set and cardinality ($K$).

analyzing the behavior of the optimal solutions in terms of the tail risk, we note that RP-CCPOP portfolios improve their control on the losses with respect to the CCPOP portfolios as $K$ increases. The proposed strategy shows a better level of diversification and lower turnover in all the experiments, analogously to the case of weekly rebalancing.

Figures 2, 3 and 4 report the evolution over the out-of-sample period of the wealth (43) for the RP-CCPOP portfolios with weekly and monthly rebalancing, denoted by RP-CCPOP$_1$ and RP-CCPOP$_4$ respectively, in comparison to the corresponding CCPOP counterparts, CCPOP$_1$ and CCPOP$_4$, and the related market index. We assume an initial wealth of 1\$ for all the portfolios. Overall, in the first two case studies, the analyzed strategies are more profitable than simply investing on the index. For the comparisons involving the data from NASDAQ 100, these strategies tend to replicate the benchmark. However, it can be noted that the number of constituents and the length of the rebalancing period affect in a different measure their performance in the three experiments.

For the DowJones data set, the top left chart in Figure 2 reveals that the strategies behave in a similar manner for small sized portfolios, irrespective to the frequency of the rebalancing. The next chart shows that CCPOP solutions do not change a lot their performance, as the cardinality increases. At the same time, RP-CCPOP$_4$ deteriorates, almost settling on the levels of the index, while the RP-CCPOP strategy with a weekly rebalancing, RP-CCPOP$_1$, guarantees the best performance, closing with a final rate of return of around 14%.

| | | NS-MOPSO | | HMOPSO* | | |
|---|---|---|---|---|---|---|
| data set | K | mean | std | mean | std | rank-sum |
| DowJones | 5 | 0.7663 | 0.0389 | 0.9810 | 0.0087 | ↓ |
| | 10 | 0.6806 | 0.0378 | 0.9784 | 0.0137 | ↓ |
| | 15 | 0.4493 | 0.1959 | 0.9999 | 0.0001 | ↓ |
| | 20 | 0.0000 | 0.0000 | 1.0000 | 0.0000 | ↓ |
| FF49Industries | 5 | 0.8636 | 0.0375 | 0.8085 | 0.0730 | ↑ |
| | 10 | 0.7799 | 0.0332 | 0.8981 | 0.0490 | ↓ |
| | 20 | 0.2977 | 0.0979 | 0.9933 | 0.0045 | ↓ |
| | 40 | 0.0000 | 0.0000 | 1.0000 | 0.0000 | ↓ |
| NASDAQ100 | 5 | 0.9217 | 0.0733 | 0.9798 | 0.0118 | ↓ |
| | 10 | 0.8257 | 0.2372 | 0.9869 | 0.0141 | ↓ |
| | 20 | 0.1772 | 0.2805 | 0.9986 | 0.0046 | ↓ |
| | 40 | 0.0342 | 0.1158 | 1.0000 | 0.0000 | ↓ |

Table 10: Mean and standard deviation values of the CR performance metric (40) for the NS-MOPSO and HMOPSO* algorithms classified by data set and cardinality ($K$). The "rank-sum" column reports the corresponding results for the Wilcoxon rank-sum test. The symbol "↑" means that NS-MOPSO has yielded better results than HMOPSO* at a 5% confidence level, "↓" indicates that the algorithm in the column is statistically better than NS-MOPSO.

RP-CCPOP$_1$ remains one of the most profitable choices, when continuing to increase the cardinality of optimal portfolios, even if it reduces the final wealth like all the other strategies. Moreover, the role of the risk parity constraint in managing extreme losses increases.

In Figure 3 we can see that the four strategies behave in a very similar way and with high profits when they are applied to the FF49Industries data set for small to medium sized portfolios. The major differences appear in the bottom right chart, where the optimal portfolios with $K = 40$ are compared. In this case, we invest in almost all the index constituents. The RP-CCPOP$_4$ solutions show a slight improvement compared to the benchmark.

Figure 4 points out the capability of the RP-CCPOP strategies to reduce the losses compared to the CCPOP strategies, especially with weekly rebalancing.

Taking into account all these findings, it could be argued that the best compromise between performance and risk control is attained by the RP-CCPOP strategy with a cardinality equal to 20%, 30% of the constituents of the market and with weekly rebalancing.

| | CCPOP | | | | RP-CCPOP | | | |
|---|---|---|---|---|---|---|---|---|
| $K$ | 5 | 10 | 15 | 20 | 5 | 10 | 15 | 20 |
| $SR$ | 0.4006 | 0.3538 | -0.0293 | 0.0728 | 0.4150 | 1.0302 | 0.6449 | 0.3836 |
| $\Omega$ | 0.7931 | 0.9084 | 0.8497 | 0.8201 | 0.8647 | 0.8389 | 0.7967 | 0.8496 |
| $MDD$ | 0.1362 | 0.1219 | 0.1486 | 0.1073 | 0.1345 | 0.0832 | 0.0549 | 0.0480 |
| $VaR_{10\%}$ | 0.0291 | 0.0282 | 0.0297 | 0.0226 | 0.0304 | 0.0208 | 0.0169 | 0.0101 |
| $CVaR_{10\%}$ | 0.0573 | 0.0539 | 0.0516 | 0.0443 | 0.0562 | 0.0349 | 0.0265 | 0.0189 |
| $DI$ | 0.0280 | 0.0312 | 0.0312 | 0.0322 | 0.0289 | 0.0328 | 0.0344 | 0.0349 |
| $turnover$ | 0.2544 | 0.5183 | 0.7180 | 0.6966 | 0.2577 | 0.5170 | 0.4668 | 0.2878 |

Table 11: Out-of-sample performance measures for the investment strategies related to CCPOP and RP-CCPOP models classified by cardinality ($K$) relative to the last 53 weeks of the DowJones data set with weekly rebalancing. "$SR$" is the annualized Sharpe ratio, "$\Omega$" is the weekly Omega ratio, "$MDD$" denotes the maximum drawdown, "$VaR_{10\%}$" and "$CVaR_{10\%}$" represent respectively the value-at-risk and the conditional value-at-risk at the 10% significance level, "$DI$" is the mean of the diversification index for the portfolio weights and "$turnover$" provides the mean turnover.

| | CCPOP | | | | RP-CCPOP | | | |
|---|---|---|---|---|---|---|---|---|
| $K$ | 5 | 10 | 20 | 40 | 5 | 10 | 20 | 40 |
| $SR$ | 2.0705 | 1.6621 | 1.2413 | 0.6384 | 2.0896 | 1.6291 | 1.0705 | 0.4317 |
| $\Omega$ | 1.6368 | 1.4159 | 1.0378 | 0.9862 | 1.5285 | 1.3914 | 0.9761 | 1.3565 |
| $MDD$ | 0.0320 | 0.0492 | 0.0551 | 0.0563 | 0.0279 | 0.0527 | 0.0592 | 0.0359 |
| $VaR_{10\%}$ | 0.0107 | 0.0158 | 0.0183 | 0.0173 | 0.0102 | 0.0194 | 0.0203 | 0.0079 |
| $CVaR_{10\%}$ | 0.0183 | 0.0207 | 0.0234 | 0.0247 | 0.0183 | 0.0225 | 0.0257 | 0.0117 |
| $DI$ | 0.0159 | 0.0179 | 0.0189 | 0.0198 | 0.0160 | 0.0180 | 0.0192 | 0.0195 |
| $turnover$ | 0.1779 | 0.3693 | 0.6267 | 0.6674 | 0.1849 | 0.3226 | 0.5494 | 0.5573 |

Table 12: Out-of-sample performance measures for the investment strategies related to CCPOP and RP-CCPOP models classified by cardinality ($K$) relative to the last 53 weeks of the FF49Industries data set with weekly rebalancing. "$SR$" is the annualized Sharpe ratio, "$\Omega$" is the weekly Omega ratio, "$MDD$" denotes the maximum drawdown, "$VaR_{10\%}$" and "$CVaR_{10\%}$" represent respectively the value-at-risk and the conditional value-at-risk at the 10% significance level, "$DI$" is the mean of the diversification index for the portfolio weights and "$turnover$" provides the mean turnover.

| | CCPOP | | | | RP-CCPOP | | | |
|---|---|---|---|---|---|---|---|---|
| $K$ | 5 | 10 | 20 | 40 | 5 | 10 | 20 | 40 |
| $SR$ | -0.3287 | -0.2462 | -0.3536 | 0.0271 | -0.0503 | -0.0603 | 0.0141 | 0.2433 |
| $\Omega$ | 0.5972 | 0.5675 | 0.5437 | 0.6848 | 0.6644 | 0.6618 | 0.6285 | 0.6872 |
| $MDD$ | 0.2423 | 0.2405 | 0.2453 | 0.1802 | 0.1943 | 0.1958 | 0.1871 | 0.1547 |
| $VaR_{10\%}$ | 0.0449 | 0.0427 | 0.0384 | 0.0410 | 0.0396 | 0.0383 | 0.0342 | 0.0382 |
| $CVaR_{10\%}$ | 0.0798 | 0.0760 | 0.0739 | 0.0697 | 0.0760 | 0.0715 | 0.0648 | 0.0663 |
| $DI$ | 0.0096 | 0.0108 | 0.0113 | 0.0119 | 0.0097 | 0.0109 | 0.0115 | 0.0119 |
| $turnover$ | 0.3299 | 0.4330 | 0.5479 | 0.5079 | 0.3465 | 0.4053 | 0.5487 | 0.5728 |

Table 13: Out-of-sample performance measures for the investment strategies related to CCPOP and RP-CCPOP models classified by cardinality ($K$) relative to the last 53 weeks of the NASDAQ100 data set with weekly rebalancing. "$SR$" is the annualized Sharpe ratio, "$\Omega$" is the weekly Omega ratio, "$MDD$" denotes the maximum drawdown, "$VaR_{10\%}$" and "$CVaR_{10\%}$" represent respectively the value-at-risk and the conditional value-at-risk at the 10% significance level, "$DI$" is the mean of the diversification index for the portfolio weights and "$turnover$" provides the mean turnover.

| | CCPOP | | | | RP-CCPOP | | | |
|---|---|---|---|---|---|---|---|---|
| $K$ | 5 | 10 | 20 | 40 | 5 | 10 | 20 | 40 |
| $SR$ | 0.4073 | 0.3253 | 0.1876 | 0.2919 | 0.2246 | 0.0584 | -0.0158 | 0.1387 |
| $\Omega$ | 0.7936 | 0.8925 | 0.7842 | 0.8160 | 0.7408 | 0.8126 | 0.8528 | 0.7168 |
| $MDD$ | 0.1372 | 0.1272 | 0.1338 | 0.1084 | 0.1387 | 0.1345 | 0.0725 | 0.0564 |
| $VaR_{10\%}$ | 0.0304 | 0.0273 | 0.0314 | 0.0276 | 0.0287 | 0.0270 | 0.0150 | 0.0119 |
| $CVaR_{10\%}$ | 0.0615 | 0.0542 | 0.0552 | 0.0504 | 0.0601 | 0.0531 | 0.0275 | 0.0220 |
| $DI$ | 0.0280 | 0.0312 | 0.0319 | 0.0317 | 0.0287 | 0.0325 | 0.0343 | 0.0350 |
| $turnover$ | 0.0734 | 0.1408 | 0.1618 | 0.1602 | 0.0744 | 0.1362 | 0.1071 | 0.0740 |

Table 14: Out-of-sample performance measures for the investment strategies related to CCPOP and RP-CCPOP models classified by cardinality ($K$) relative to the last 53 weeks of the DowJones data set with monthly rebalancing. "$SR$" is the annualized Sharpe ratio, "$\Omega$" is the weekly Omega ratio, "$MDD$" denotes the maximum drawdown, "$VaR_{10\%}$" and "$CVaR_{10\%}$" represent respectively the value-at-risk and the conditional value-at-risk at the 10% significance level, "$DI$" is the mean of the diversification index for the portfolio weights and "$turnover$" provides the mean turnover.

| | CCPOP | | | | RP-CCPOP | | | |
|---|---|---|---|---|---|---|---|---|
| $K$ | 5 | 10 | 20 | 40 | 5 | 10 | 20 | 40 |
| $SR$ | 1.8358 | 1.4360 | 1.2331 | 0.3629 | 1.9389 | 1.6371 | 0.9724 | 1.1034 |
| $\Omega$ | 1.3864 | 1.2955 | 1.2148 | 0.9001 | 1.3294 | 1.3932 | 1.0200 | 1.3740 |
| $MDD$ | 0.0375 | 0.0505 | 0.0607 | 0.0689 | 0.0376 | 0.0411 | 0.0599 | 0.0209 |
| $VaR_{10\%}$ | 0.0139 | 0.0185 | 0.0198 | 0.0234 | 0.0127 | 0.0150 | 0.0212 | 0.0087 |
| $CVaR_{10\%}$ | 0.0194 | 0.0216 | 0.0247 | 0.0273 | 0.0188 | 0.0209 | 0.0253 | 0.0115 |
| $DI$ | 0.0159 | 0.0180 | 0.0189 | 0.0199 | 0.0159 | 0.0180 | 0.0192 | 0.0196 |
| *turnover* | 0.0665 | 0.0831 | 0.1607 | 0.1496 | 0.0814 | 0.1020 | 0.1402 | 0.1281 |

Table 15: Out-of-sample performance measures for the investment strategies related to CCPOP and RP-CCPOP models classified by cardinality ($K$) relative to the last 53 weeks of the FF49Industries data set with monthly rebalancing. "$SR$" is the annualized Sharpe ratio, "$\Omega$" is the weekly Omega ratio, "$MDD$" denotes the maximum drawdown, "$VaR_{10\%}$" and "$CVaR_{10\%}$" represent respectively the value-at-risk and the conditional value-at-risk at the 10% significance level, "$DI$" is the mean of the diversification index for the portfolio weights and "*turnover*" provides the mean turnover.

| | CCPOP | | | | RP-CCPOP | | | |
|---|---|---|---|---|---|---|---|---|
| $K$ | 5 | 10 | 20 | 40 | 5 | 10 | 20 | 40 |
| $SR$ | -0.3944 | -0.2395 | -0.1957 | 0.1566 | -0.2690 | -0.0820 | 0.0827 | 0.1607 |
| $\Omega$ | 0.6301 | 0.6681 | 0.6272 | 0.6121 | 0.7145 | 0.6560 | 0.7574 | 0.6656 |
| $MDD$ | 0.3043 | 0.2532 | 0.2458 | 0.1749 | 0.2733 | 0.2198 | 0.1853 | 0.1599 |
| $VaR_{10\%}$ | 0.0475 | 0.0410 | 0.0429 | 0.0389 | 0.0402 | 0.0439 | 0.0355 | 0.0402 |
| $CVaR_{10\%}$ | 0.0850 | 0.0763 | 0.0743 | 0.0701 | 0.0853 | 0.0753 | 0.0671 | 0.0669 |
| $DI$ | 0.0096 | 0.0108 | 0.0114 | 0.0119 | 0.0097 | 0.0109 | 0.0115 | 0.0119 |
| *turnover* | 0.1511 | 0.1146 | 0.1593 | 0.1361 | 0.1472 | 0.1216 | 0.1486 | 0.1454 |

Table 16: Out-of-sample performance measures for the investment strategies related to CCPOP and RP-CCPOP models classified by cardinality ($K$) relative to the last 53 weeks of the NASDAQ100 data set with monthly rebalancing. "$SR$" is the annualized Sharpe ratio, "$\Omega$" is the weekly Omega ratio, "$MDD$" denotes the maximum drawdown, "$VaR_{10\%}$" and "$CVaR_{10\%}$" represent respectively the value-at-risk and the conditional value-at-risk at the 10% significance level, "$DI$" is the mean of the diversification index for the portfolio weights and "*turnover*" provides the mean turnover.

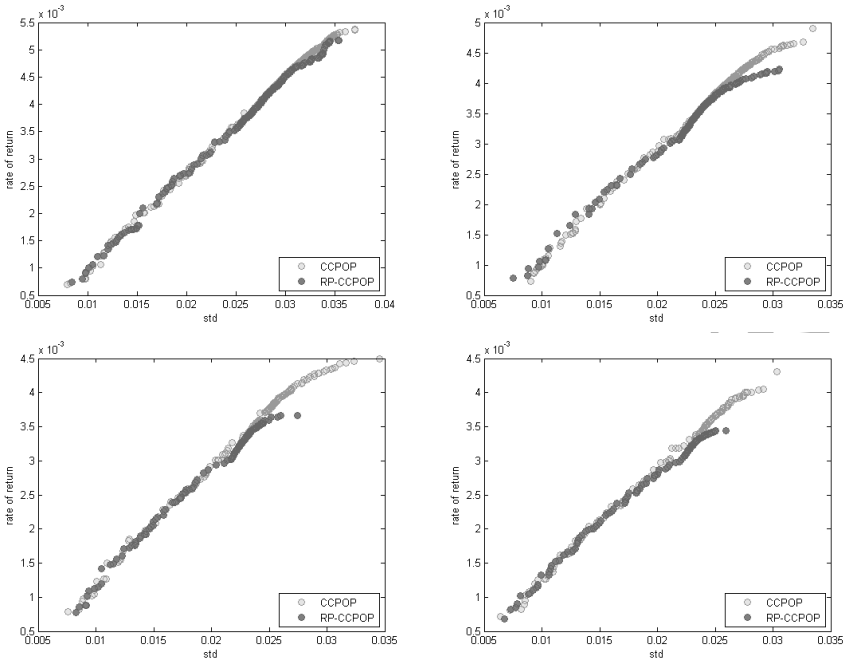


Figure 1: Efficient frontiers for CCPOP and RP-CCPOP models related to the DowJones data set with $K$ in $\{5, 10, 15, 20\}$. The top left chart refers to portfolios with cardinality $K = 5$, the top right displays portfolios with $K = 10$, the remaining plots regard solutions with $K = 15$ (on the left) and with $K = 20$ (on the right), respectively.

## 6. Conclusions

We have proposed an extension of the Markowitz mean-variance asset allocation framework, where cardinality, buy-in thresholds, budget constraints and risk parity conditions are handled at the same time. The resulting mixed-integer bi-objective portfolio optimization problem has been tackled by means of a novel version of the multi-objective particle swarm optimization algorithm, called HMOPSO. This uses a swap mutation operator to improve the exploration capabilities of the original algorithm, and handles the constraints by a hybrid technique that combines a repair mechanism with different instances of the domination principle.

The computational analysis on a set of real-world test problems confirms the effectiveness and the robustness of HMOPSO. In particular, the variant using a self-adaptive tolerance for relaxing the risk parity condition provides the best compromise between the quality of solutions produced and the number of optimal risk-return profiles identified on the approximated Pareto front. Additional investigations, concerning the standard cardinality constrained portfolio optimization, have highlighted the benefits of the novel optimization strategy for

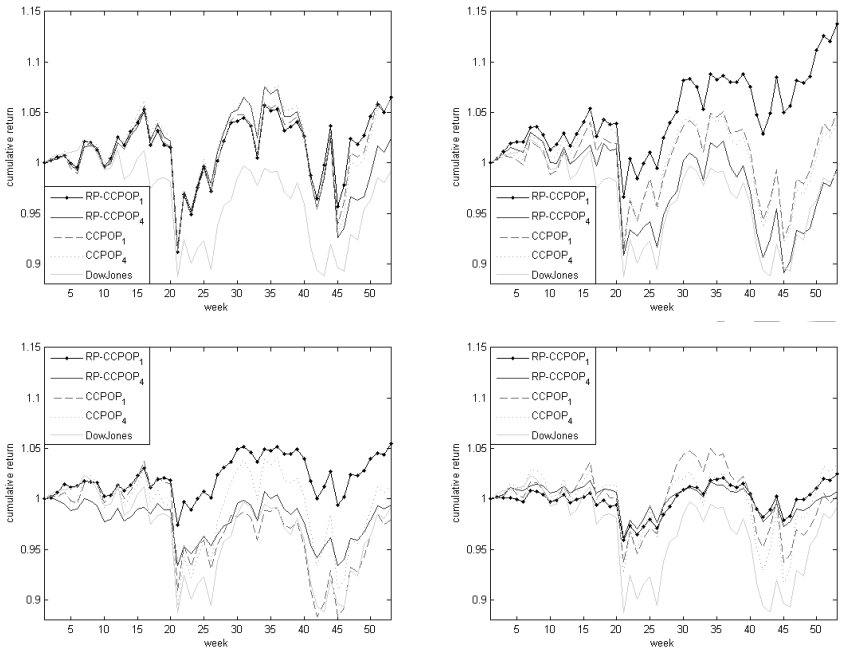


Figure 2: Out-of-sample evolution of the wealth for the portfolios related to CCPOP and RP-CCPOP models over the last 53 weeks of the DowJones data set, taking into account weekly and monthly rebalancing strategies. The top left chart refers to portfolios with cardinality $K = 5$, the top right displays portfolios with $K = 10$, the remaining plots regard solutions with $K = 15$ (on the left) and with $K = 20$ (on the right), respectively.

risk management purposes. Indeed, the combination of cardinality constraint and risk parity permits to simultaneously control costs and risk contributions. The resulting portfolios present losses which are consistently reduced. At the same time, profits are comparable, or even higher, with respect to the portfolios optimized in terms of the standard cardinality constrained mean-variance model over all the out-of-sample period.

In our future research, we plan to study the performance of other bio-inspired algorithms and constraint-handling techniques for the RP-CCPOP. At the same time, it will be interesting to study the influence of different risk measures on the structure of the investible portfolios, when risk parity is included as a constraint.

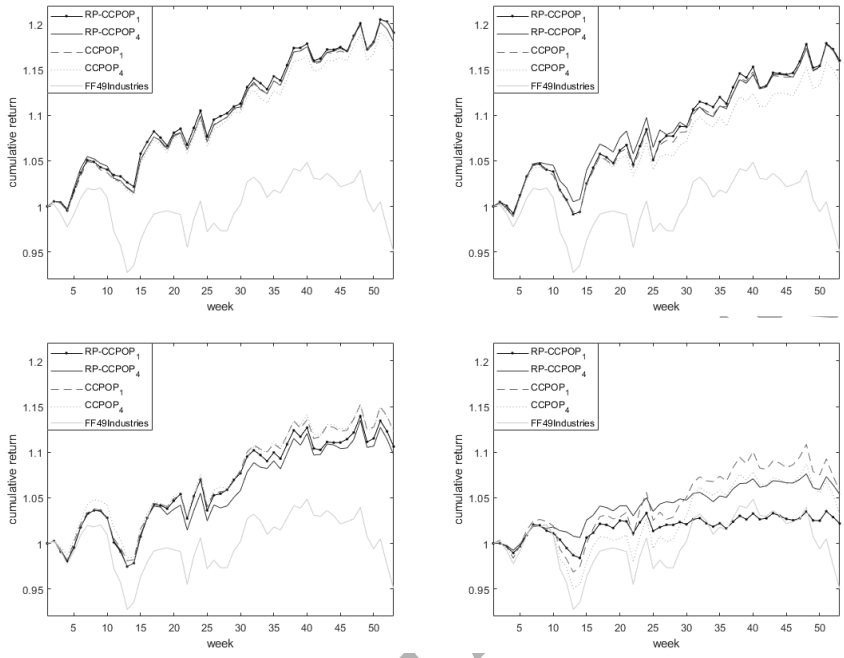


Figure 3: Out-of-sample evolution of the wealth for the portfolios related to CCPOP and RP-CCPOP models over the last 53 weeks of the FF49Industries data set, taking into account weekly and monthly rebalancing strategies. The top left chart refers to portfolios with cardinality $K = 5$, the top right displays portfolios with $K = 10$, the remaining plots regard solutions with $K = 20$ (on the left) and with $K = 40$ (on the right), respectively.

## List of acronyms and abbreviations

The following acronyms and abbreviations are used in the text:

| | |
|---|---|
| CCPOP | cardinality constrained portfolio optimization problem |
| RP-CCPOP | risk parity based cardinality constrained portfolio optimization problem |
| MOPSO | multi-objective particle swarm optimization |
| HMOPSO | proposed version of MOPSO using a hybrid constraint-handling technique |
| HMOPSO* | HMOPSO modification to solve cardinality constrained portfolio optimization problems |
| NS-MOPSO | non-dominated sorting multi-objective particle swarm optimization |
| $h$ | Herfindahl index of risk contributions |
| $HV$ | hypervolume |
| $CR$ | contribution rate |
| $SR$ | Sharpe ratio |
| $\Omega$ | Omega ratio |
| $MDD$ | maximum drawdown |
| $VaR_{10\%}$ | value-at-risk at the 10% significance level |
| $CVaR_{10\%}$ | conditional value-at-risk at the 10% significance level |
| $DI$ | average of the diversification index |

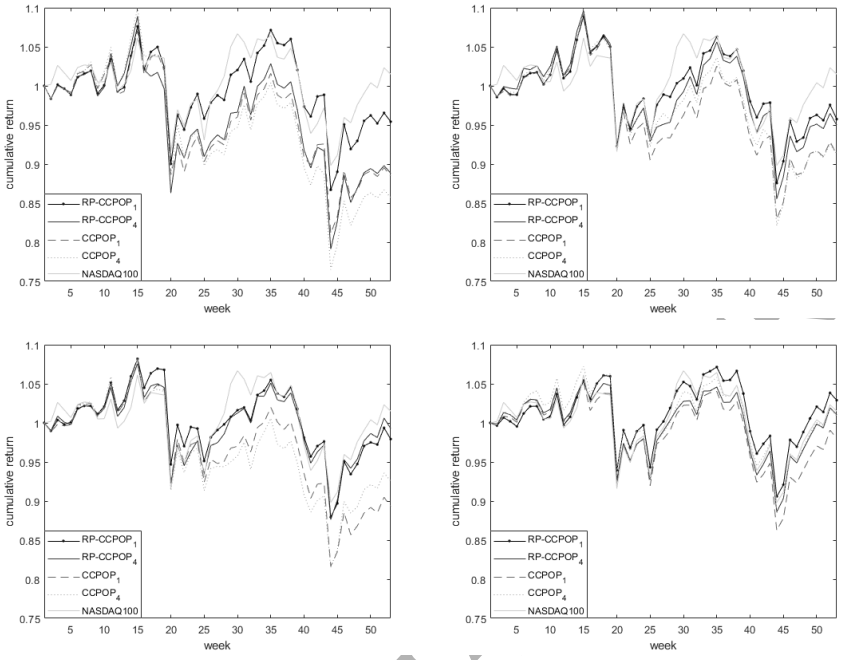


Figure 4: Out-of-sample evolution of the wealth for the portfolios related to CCPOP and RP-CCPOP models over the last 53 weeks of the NASDAQ100 data set, taking into account weekly and monthly rebalancing strategies. The top left chart refers to portfolios with cardinality $K = 5$, the top right displays portfolios with $K = 10$, the remaining plots regard solutions with $K = 20$ (on the left) and with $K = 40$ (on the right), respectively.

## References

## References

[1] H. Markowitz, Portfolio selection, The Journal of Finance 7 (1) (1952) 77–91.

[2] J. B. Guerard Jr, Handbook of portfolio construction: contemporary applications of Markowitz techniques, Springer Science & Business Media, 2009.

[3] P. N. Kolm, R. Tütüncü, F. J. Fabozzi, 60 years of portfolio optimization: practical challenges and current trends, European Journal of Operational Research 234 (2) (2014) 356–371.

[4] K. Liagkouras, K. Metaxiotis, Efficient portfolio construction with the use of multiobjective evolutionary algorithms: best practices and performance metrics, International Journal of Information Technology & Decision Making 14 (3) (2015) 535–564.

[5] R. Moral-Escudero, R. Ruiz-Torrubiano, A. Suárez, Selection of optimal investment portfolios with cardinality constraints, in: Evolutionary Computation, 2006. CEC 2006. IEEE Congress on, IEEE, 2006, pp. 2382–2388.

[6] D. Li, X. Sun, J. Wang, Optimal lot solution to cardinality constrained mean–variance formulation for portfolio selection, Mathematical Finance 16 (1) (2006) 83–101.

[7] D. X. Shaw, S. Liu, L. Kopman, Lagrangian relaxation procedure for cardinality-constrained portfolio optimization, Optimisation Methods & Software 23 (3) (2008) 411–420.

[8] D. Bertsimas, R. Shioda, Algorithm for cardinality-constrained quadratic optimization, Computational Optimization and Applications 43 (1) (2009) 1–22.

[9] T.-J. Chang, N. Meade, J. E. Beasley, Y. M. Sharaiha, Heuristics for cardinality constrained portfolio optimisation, Computers & Operations Research 27 (13) (2000) 1271–1302.

[10] N. J. Jobst, M. D. Horniman, C. A. Lucas, G. Mitra, Computational aspects of alternative portfolio selection models in the presence of discrete asset choice constraints, Quantitative Finance 1 (5) (2001) 489–501.

[11] Y. Crama, M. Schyns, Simulated annealing for complex portfolio selection problems, European Journal of Operational Research 150 (3) (2003) 546–571.

[12] T. Cura, Particle swarm optimization approach to portfolio optimization, Nonlinear Analysis: Real World Applications 10 (4) (2009) 2396–2406.

[13] M. Woodside-Oriakhi, C. Lucas, J. E. Beasley, Heuristic algorithms for the cardinality constrained efficient frontier, European Journal of Operational Research 213 (3) (2011) 538–550.

[14] P. Mutunge, D. Haugland, Minimizing the tracking error of cardinality constrained portfolios, Computers & Operations Research 90 (2018) 33–41.

[15] K. P. Anagnostopoulos, G. Mamanis, A portfolio optimization model with three objectives and discrete variables, Computers & Operations Research 37 (7) (2010) 1285–1297.

[16] K. P. Anagnostopoulos, G. Mamanis, The mean–variance cardinality constrained portfolio optimization problem: an experimental evaluation of five multiobjective evolutionary algorithms, Expert Systems with Applications 38 (11) (2011) 14208–14217.

[17] K. Liagkouras, K. Metaxiotis, Examining the effect of different configuration issues of the multiobjective evolutionary algorithms on the efficient frontier formulation for the constrained portfolio optimization problem, Journal of the Operational Research Society (2017) 1–23.

[18] P. Artzner, F. Delbaen, J.-M. Eber, D. Heath, Coherent measures of risk, Mathematical finance 9 (3) (1999) 203–228.

[19] R. T. Rockafellar, S. Uryasev, et al., Optimization of conditional value-at-risk, Journal of risk 2 (2000) 21–42.

[20] T. Roncalli, Introduction to risk parity and budgeting, CRC Press, 2013.

[21] D. Chaves, J. Hsu, F. Li, O. Shakernia, Risk parity portfolio vs. other asset allocation heuristic portfolios, The Journal of Investing 20 (1) (2011) 108–118.

[22] E. Qian, On the financial interpretation of risk contribution: risk budgets do add up, Journal of Investment Management 4 (4) (2006) 41–51.

[23] S. Maillard, T. Roncalli, J. Teïletche, The properties of equally weighted risk contribution portfolios, The Journal of Portfolio Management 36 (4) (2010) 60–70.

[24] M. D. Braga, Risk parity versus other $\mu$-free strategies: a comparison in a triple view, Investment Management and Financial Innovations 12 (2) (2015) 277–289.

[25] T. Griveau-Billion, J.-C. Richard, T. Roncalli, A fast algorithm for computing high-dimensional risk parity portfolios, available at SSRN: https://ssrn.com/abstract=2325255 (September 2013).

[26] F. Spinu, An algorithm for computing risk parity weights, available at SSRN: https://ssrn.com/abstract=2297383 (July 2013).

[27] X. Bai, K. Scheinberg, R. Tutuncu, Least-squares approach to risk parity in portfolio selection, Quantitative Finance 16 (3) (2016) 357–376.

[28] G. Vijayalakshmi Pai, T. Michel, Metaheuristic optimization of marginal risk constrained long-short portfolios, Journal of Artificial Intelligence and Soft Computing Research 2 (3) (2012) 259–274.

[29] R. Hochreiter, An evolutionary optimization approach to risk parity portfolio selection, in: European Conference on the Applications of Evolutionary Computation, Springer, 2015, pp. 279–288.

[30] T. Roncalli, Introducing expected returns into risk parity portfolios: a new framework for asset allocation, available at SSRN: https://ssrn.com/abstract=2321309 (April 2014).

[31] P. Tseng, Convergence of a block coordinate descent method for nondifferentiable minimization, Journal of Optimization Theory and Applications 109 (3) (2001) 475–494.

[32] Y. Feng, D. P. Palomar, SCRIP: successive convex optimization methods for risk parity portfolio design, IEEE Transactions on Signal Processing 63 (19) (2015) 5285–5300.

[33] Y. Feng, D. P. Palomar, Portfolio optimization with asset selection and risk parity control, in: Acoustics, Speech and Signal Processing (ICASSP), 2016 IEEE International Conference on, IEEE, 2016, pp. 6585–6589.

[34] R. L. de Carvalho, X. Lu, P. Moulin, Demystifying equity risk–based strategies: a simple alpha plus beta description, The Journal of Portfolio Management 38 (3) (2012) 56–70.

[35] R. L. de Carvalho, X. Lu, P. Moulin, An integrated risk-budgeting approach for multi-strategy equity portfolios, Journal of Asset Management 15 (1) (2014) 24–47.

[36] F. Siu, Risk parity strategies for equity portfolio management: can an asset-class strategy translate to equities?, Journal of Indexes (2014) 18–25.

[37] C. A. C. Coello, G. T. Pulido, M. S. Lechuga, Handling multiple objectives with particle swarm optimization, IEEE Transactions on Evolutionary Computation 8 (3) (2004) 256–279.

[38] K. Deb, An efficient constraint handling method for genetic algorithms, Computer Methods in Applied Mechanics and Engineering 186 (2) (2000) 311–338.

[39] H. Zhang, G. Rangaiah, An efficient constraint handling method with integrated differential evolution for numerical and engineering optimization, Computers & Chemical Engineering 37 (2012) 74–88.

[40] Y. G. Woldesenbet, G. G. Yen, B. G. Tessema, Constraint handling in multiobjective evolutionary optimization, IEEE Transactions on Evolutionary Computation 13 (3) (2009) 514–525.

[41] F. Streichert, H. Ulmer, A. Zell, Evaluating a hybrid encoding and three crossover operators on the constrained portfolio selection problem, in: Evolutionary Computation, 2004. CEC2004. Congress on, Vol. 1, IEEE, 2004, pp. 932–939.

[42] S. B. Yaakob, J. Watada, A hybrid particle swarm optimization approach to mixed integer quadratic programming for portfolio selection problems, International Journal of Simulation–Systems, Science & Technology 11 (5).

[43] S. K. Mishra, G. Panda, R. Majhi, A comparative performance assessment of a set of multiobjective algorithms for constrained portfolio assets selection, Swarm and Evolutionary Computation 16 (2014) 38–51.

[44] J. J. Liang, B.-Y. Qu, Large-scale portfolio optimization using multiobjective dynamic mutli-swarm particle swarm optimizer, in: Swarm Intelligence (SIS), 2013 IEEE Symposium on, IEEE, 2013, pp. 1–6.

[45] J. E. Beasley, Portfolio optimisation: models and solution approaches, in: Theory Driven by Influential Applications, INFORMS, 2013, pp. 201–221.

[46] H. Kaya, W. Lee, Demystifying risk parity, available at SSRN: https://ssrn.com/abstract=1987770 (January 2012).

[47] R. Eberhart, J. Kennedy, A new optimizer using particle swarm theory, in: Micro Machine and Human Science, 1995. MHS'95., Proceedings of the Sixth International Symposium on, IEEE, 1995, pp. 39–43.

[48] O. Ertenlice, C. B. Kalayci, A survey of swarm intelligence for portfolio optimization: Algorithms and applications, Swarm and evolutionary computation 39 (2018) 36–52.

[49] F. Xu, W. Chen, Stochastic portfolio selection based on velocity limited particle swarm optimization, in: Intelligent Control and Automation, 2006. WCICA 2006. The Sixth World Congress on, Vol. 1, IEEE, 2006, pp. 3599–3603.

[50] S. S. Meghwani, M. Thakur, Multi-criteria algorithms for portfolio optimization under practical constraints, Swarm and Evolutionary Computation 37 (2017) 104–125.

[51] H. Ishibuchi, K. Doi, Y. Nojima, On the effect of normalization in MOEA/D for multi-objective and many-objective optimization, Complex & Intelligent Systems 3 (4) (2017) 279–294.

[52] C. M. Fonseca, J. D. Knowles, L. Thiele, E. Zitzler, A tutorial on the performance assessment of stochastic multiobjective optimizers, in: Third International Conference on Evolutionary Multi-Criterion Optimization (EMO 2005), Vol. 216, 2005, p. 240.

[53] E. Zitzler, L. Thiele, Multiobjective optimization using evolutionary algorithmsa comparative case study, in: International conference on parallel problem solving from nature, Springer, 1998, pp. 292–301.

[54] E. Zitzler, D. Brockhoff, L. Thiele, The hypervolume indicator revisited: On the design of pareto-compliant indicators via weighted integration, in: International Conference on Evolutionary Multi-Criterion Optimization, Springer, 2007, pp. 862–876.

[55] M. Li, S. Yang, X. Liu, A performance comparison indicator for pareto front approximations in many-objective optimization, in: Proceedings of the 2015 Annual Conference on Genetic and Evolutionary Computation, ACM, 2015, pp. 703–710.

[56] A. Auger, J. Bader, D. Brockhoff, E. Zitzler, Theory of the hypervolume indicator: optimal $\mu$-distributions and the choice of the reference point, in: Proceedings of the tenth ACM SIGEVO workshop on Foundations of genetic algorithms, ACM, 2009, pp. 87–102.

[57] G. L. Lizárraga, On the evaluation of the quality of non-dominated sets, Ph.D. thesis, Ph. D. thesis, Centro de Investigación en Matemáticas, AC (CIMAT) (2009).

[58] Y. Cao, B. J. Smucker, T. J. Robinson, On using the hypervolume indicator to compare pareto fronts: Applications to multi-criteria optimal experimental design, Journal of Statistical Planning and Inference 160 (2015) 60–74.

[59] W. F. Sharpe, Mutual fund performance, The Journal of business 39 (1) (1966) 119–138.

[60] C. Keating, W. F. Shadwick, A universal performance measure, Journal of performance measurement 6 (3) (2002) 59–84.

[61] W. Woerheide, D. Persson, An index of portfolio diversification, Financial services review 2 (2) (1993) 73–85.

[62] V. DeMiguel, L. Garlappi, R. Uppal, Optimal versus naive diversification: How inefficient is the 1/n portfolio strategy?, The review of Financial studies 22 (5) (2007) 1915–1953.

[63] R. Bruni, F. Cesarone, A. Scozzari, F. Tardella, Real-world datasets for portfolio selection and solutions of some stochastic dominance portfolio models, Data in Brief 8 (2016) 858–862.

[64] A. E. Eiben, S. K. Smit, Parameter tuning for configuring and analyzing evolutionary algorithms, Swarm and Evolutionary Computation 1 (1) (2011) 19–31.

[65] K. Lwin, R. Qu, G. Kendall, A learning-guided multi-objective evolutionary algorithm for constrained portfolio optimization, Applied Soft Computing 24 (2014) 757–772.

[66] S. G. Eakins, S. Stansell, An examination of alternative portfolio rebalancing strategies applied to sector funds, Journal of Asset Management 8 (1) (2007) 1–8.